Published in final edited form as:

J Immunol. 2019 December 01; 203(11): 2928–2943. doi:10.4049/jimmunol.1900792.

Role of IL-15 Signaling in the Pathogenesis of Simian Immunodeficiency Virus Infection in Rhesus Macaques

Afam A. Okoye[*,†], **Maren Q. DeGottardi**[*,†], **Yoshinori Fukazawa**[*,†], **Mukta Vaidya**[*,†], **Chike O. Abana**[*,†], **Audrie L. Konfe**[*,†], **Devin N. Fachko**[*,†], **Derick M. Duell**[*,†], **He Li**[*,†], **Richard Lum**[*,†], **Lina Gao**[‡], **Byung S. Park**[‡], **Rebecca L. Skalsky**[*,†], **Anne D. Lewis**[†], **Michael K. Axthelm**[*,†], **Jeffrey D. Lifson**[§], **Scott W. Wong**[*,†], **Louis J. Picker**[*,†]

[*]Vaccine and Gene Therapy Institute, Oregon Health & Science University, Beaverton, OR 97006

[†]Oregon National Primate Research Center, Oregon Health & Science University, Beaverton, OR 97006

[‡]Division of Biostatistics, Department of Public Health and Preventative Medicine, Oregon Health & Science University, Portland, OR, 97239

[§]AIDS and Cancer Virus Program, Leidos Biomedical Research, Inc., Frederick National Laboratory, Frederick, MD, 21702.

Abstract

Although IL-15 has been implicated in the pathogenic hyperimmune activation that drives progressive HIV and SIV infection, as well as in the generation of HIV/SIV target cells, it also supports NK and T cell homeostasis and effector activity, potentially benefiting the host. To understand the role of IL-15 in SIV infection and pathogenesis, we treated two cohorts of SIVmac239-infected rhesus macaques (*Macaca mulatta*; RM), one with chronic infection, the other with primary infection, with a rhesusized, IL-15-neutralizing mAb (vs. an IgG isotype control) for up to 10 weeks (n = 7–9 RM per group). In both cohorts, anti-IL-15 was highly efficient at blocking IL-15 signaling *in vivo*, causing 1) profound depletion of NK cells in blood and tissues throughout the treatment period, 2) substantial, albeit transient, depletion of $CD8^+$ effector memory T cells (but not the naïve and central memory subsets), and 3) $CD4^+$ and $CD8^+$ effector memory T cell hyperproliferation. In primary infection, reduced frequencies of SIV-specific effector T cells in an extra-lymphoid tissue site were also observed. Despite these effects, the kinetics and extent of SIV replication, $CD4^+$ T cell depletion, and the onset of AIDS were comparable between anti-IL-15- and control-treated groups in both cohorts. However, RM treated with anti-IL-15 during primary infection manifested accelerated reactivation of rhesus macaque rhadinovirus. Thus, IL-15 support of NK cell and effector memory T cell homeostasis does not play a demonstrable, non-redundant role in SIV replication or $CD4^+$ T cell deletion dynamics, but may contribute to immune control of oncogenic γ-herpesviruses.

Correspondence to: Louis J. Picker, M.D., Vaccine and Gene Therapy Institute, Oregon Health & Science University – West Campus, 505 NW 185th Ave., Beaverton, OR 97006, PHN: (503) 418-2720; FAX: (503) 418-2701, pickerl@ohsu.edu.

Disclosures: None of the authors have financial conflicts of interest related to this work.

INTRODUCTION

The homeostatic cytokine IL-15 is produced by numerous cell types in diverse tissues, in particular monocytes/macrophages and dendritic cells, and its expression can be upregulated by inflammatory signaling, including ligation of toll-like receptors with their ligands or induction of type I interferon (1–4). IL-15 signals through the common γ-chain receptor cytokine family and provides survival and differentiation signals involved with the development and maintenance of NK cell and memory T cell (T_M) homeostasis and function (4–9). Due to its ability to enhance the production, homeostasis and functional (effector) activity of various lymphoid effector populations, IL-15 is currently under investigation as a therapeutic option in a number of disease conditions, such as viral infections (6, 10), immune reconstitution (11) and cancer (7, 8). IL-15 is upregulated during HIV and SIV infection and its activity may support anti-viral immunity by: 1) enhancing the activation of innate immune effectors, such as NK cells, early after infection; 2) promoting the generation, expansion and maintenance of HIV/SIV-specific $CD8^+$ T cell responses (12); and 3) promoting the expansion and differentiation of viral infection-depleted $CD4^+$, $CCR5^+$ transitional (T_{TrM}) and effector (T_{EM}) memory T cells from their $CCR5^-$ naïve (T_N) and/or central memory (T_{CM}) precursors, providing for reconstitution of the depleted populations (13, 14).

Exogenous IL-15 administration in both nonhuman primates (NHP) and humans results in selective induction of proliferation among $CD4^+$ and $CD8^+$ T_M cells with effector differentiation (T_{EM} and T_{TrM}) (15–18). This suggests that IL-15 can stimulate the expansion of antigen-specific effector T cell populations and supports the use of IL-15 as an adjuvant to boost immune response against HIV/SIV. Indeed, administration of the IL-15 superagonist ALT-803 to SIV-infected RM was shown to enhance SIV-specific T cell responses, reduce plasma viral loads (pvl) and even direct SIV-specific T cells into B cell follicles (19, 20). Similarly, there was an increase in SIV-specific $CD8^+$ T cells with granzyme B expression and a decrease in viral RNA in lymph nodes of simian/human immunodeficiency virus (SHIV)-infected RM after treatment with heterodimeric IL-15, a stable noncovalent complex of IL-15 and the IL-15 receptor α chain (21). IL-15 can also induce the proliferative expansion and migration of both $CD4^+$ and $CD8^+$ T_{EM}/T_{TrM} from the periphery into extra lymphoid effector sites in RM (17). Collectively, these studies suggest that modulation of IL-15 signaling may be an effective therapeutic approach to enhance control of virus replication and/or to support immune reconstitution post-infection (pi).

However, despite the potential beneficial effect of IL-15-mediated expansion of anti-viral $CD8^+$ effectors and $CD4^+$ T_M cells in facilitating control of HIV/SIV infection and $CD4^+$ T cell reconstitution, respectively, several lines of evidence suggest IL-15 activity may also potentiate HIV/SIV disease progression. Plasma isolated during acute HIV infection revealed that the level of certain plasma cytokines predicted 66% of variation in pvl, with IL-15 levels significantly associated with higher pvl set points (22). In untreated HIV-infected patients with pvl above 100,000 copies/ml, IL-15 levels also strongly correlate with increasing HIV-1 viremia (23). IL-15 administration to RM during acute SIV infection was associated with enhanced activation and proliferation of $CD4^+$ T_M, higher post-peak virus

replication set points and accelerated disease progression despite higher SIV-specific $CD8^+$ T cell responses (24). Although the precise mechanisms by which IL-15 administration appears to enhance rates of virus replication are unclear, IL-15-mediated up-regulation of the HIV/SIV receptor CD4 (25), and/or co-receptor CCR5 (26) might increase target cell susceptibility and/or number. It has also been suggested that overexposure of developing virus-specific T cells to IL-15 might compromise the generation and/or long-term stability of effector $CD8^+$ T cell responses, which could account for the increased pvl observed in animals treated with IL-15 during acute SIV infection (27). Finally, elevated IL-15 levels during HIV/SIV infection could have an overall negative impact on $CD4^+$ T cell homeostasis. Indeed, we have shown that IL-15 supports the homeostatic maintenance of $CD4^+$ T_{TrM} and T_{EM} *in vivo*, and can induce $CD4^+$ T_{CM} to simultaneously proliferate and differentiate into T_{EM} *in vitro* (26). As such, long-term exposure of $CD4^+$ T_{CM} to elevated levels of IL-15 during HIV/SIV infection might disturb the balance between $CD4^+$ T_{CM} self-renewal and $CD4^+$ T_{CM} differentiation into T_{EM}, promoting population failure by inducing excessive differentiation and ultimately contributing to the collapse of $CD4^+$ T_{CM} homeostasis and overt immunodeficiency (13).

IL-15 signaling is also a primary regulator of NK cell homeostasis and function, and in fact, this cytokine is essential for peripheral maintenance of NK cells (4, 26, 28). Therefore, to the extent that NK cells contribute to the control of HIV/SIV replication, IL-15 would be required for this activity. However, the contribution of NK cells in the control of HIV/SIV replication remains controversial. Recent data suggests that expression of human leukocyte antigen A (HLA-A) may impair control of HIV infection through the inhibition of NKG2A-mediated NK cell licensing (29), suggesting NK cells may play a role in viral control. Previous work evaluating the role of NK cells in the SIV-RM model involved the use of a depleting anti-CD16 mAb administered during primary SIV infection (30). Although NK cell depletion was incomplete, the partial depletion in peripheral blood $CD16^+$ NK cells achieved was associated with no demonstrable effect on pvl or kinetics of $CD4^+$ T cell depletion (31). In contrast, control of SIV replication in lymph node (LN) B cell follicles by NK cells was associated with high levels of local expression of IL-15 in African green monkeys and distinguishes SIV infection of African green monkeys from pathogenic SIV infection of RM (32).

In this study, we sought to better define the role of IL-15-dependent immune regulation in acute and chronic SIV infection by specifically inhibiting IL-15 activity *in vivo* using a rhesusized anti-IL-15 mAb that we have previously shown selectively abrogates IL-15 signaling in RM (26). If IL-15-dependent NK cell and/or $CD8^+$ T cell effector responses were essential for SIV control, we would expect anti-IL-15 mAb-treated RM to exhibit enhanced viral replication and rapid disease progress relative to controls. On the other hand, if $CD4^+$ T_M regeneration was a dominant effect of IL-15, reduced IL-15 might be expected to initially reduce viral loads due to accelerated $CD4^+$ target cell depletion, but at the same time hasten disease pathogenesis by facilitating collapse of $CD4^+$ T_M populations (13). Instead, we found that despite the profound loss of NK cells and significant perturbations in T_{EM} homeostasis, the magnitude and kinetics of SIV replication, $CD4^+$ T cell depletion, and overall SIV disease progression were not significantly different between anti-IL-15-treated RM versus controls. However, prolonged anti-IL-15 mAb treatment during primary SIV

infection did accelerate reactivation of rhesus macaque rhadinovirus (RRV), a simian γ-herpesvirus closely related to human herpesvirus type 8 (HHV8)/Kaposi's sarcoma-associated herpesvirus (KSHV) (33, 34). We also observed cases of non-Hodgkin's lymphoma (NHL) in anti-IL-15-treated RM that were predominantly associated with lymphocryptovirus (LCV), the simian homologue of EBV (35, 36). Collectively, these data suggest that while IL-15 signaling is not a primary regulator of SIV pathogenesis, it may play an important role in maintaining immune control of oncogenic γ−herpesviruses in SIV-infected immunodeficient RM.

MATERIALS AND METHODS

Animals

A total of 55 purpose-bred male and female RM (*Macaca mulatta*) of Indian genetic background and free of Macacine alphaherpesvirus 1, D type simian retrovirus and Primate T-lymphotrophic virus 1 were used in this study. For chronic SIV infection studies, a subgroup of 18 SIVmac239-infected RM (between 196 – 565 days post-SIV infection) was administered the rhesus recombinant anti-IL-15 mAb, clone M111 (n = 9) or a rhesus recombinant IgG control mAb (n = 9), i.v. once every 2 weeks at 20mg/kg on day 0 and 10mg/kg on days 14, 28, 42, 56 and 70. A subgroup of 14 SIV naive RM were used as uninfected controls. For primary SIV infection studies, 23 RM were intra-rectally inoculated with 3000 $TCID_{50}$ of SIVmac239. Of these, a subgroup of 7 RM was administered anti-IL-15 mAb, i.v. once every 2 weeks at 20mg/kg on day −42 and at 10mg/kg on days −28 and −14 prior to SIV infection (Group A). Another subgroup of 16 RM was administered with anti-IL-15 mAb (n = 8) (Group B) or IgG control mAb (n = 8) (Group C), i.v. once every 2 weeks at 20mg/kg on day −42 and at 10mg/kg on days −28 and −14 prior to SIV infection, and 10mg/kg on days 0, 14, 28, 42 and 56 after SIV challenge. BrdU (Sigma-Aldrich) was prepared and administered i.v. in three separate doses of 30mg/kg body weight over a 24-hour period on day 40–41 pi as previously described (26). All RM were housed at the Oregon National Primate Research Center in accordance with standards of the Center's Institutional Animal Care and Use Committee and the National Institutes of Health Guide for the Care and Use of Laboratory Animals

Flow cytometric analysis

Whole blood and mononuclear cells isolated from lymph nodes (LN), bronchoalveolar lavage (BAL or lung airspace), bone marrow and small intestinal mucosa were obtained and stained for flow cytometric analysis as previously described (13, 17, 27). Polychromatic (8- to 12-parameter) flow cytometric analysis was performed on an LSR II instrument (BD Biosciences) using Pacific Blue, AmCyan, FITC, PE, PE-Texas Red, PE-Cy7, PerCP-Cy5.5, allophycocyanin, allophycocyanin-Cy7, and Alexa Fluor 700 as the available fluorescent parameters. List mode multiparameter data files were analyzed using FlowJo software (Tree Star). Delineation of T_N and T_M subsets and for setting + versus − markers for CCR5 and Ki-67 expression have been previously described in detail (13, 17, 27). Briefly, for each subset to be quantified, the percentages of the subset within the overall small lymphocyte and/or small T cell ($CD3^+$ small lymphocyte) populations were determined. For quantification of peripheral blood subsets, absolute small lymphocyte counts were obtained

using an AcT5diff cell counter (Beckman Coulter) and, from these values, absolute counts for the relevant subset were calculated based on the subset percentages within the light scatter–defined small lymphocyte population on the flow cytometer. Baseline values were determined as the average of values at days −14, −7, and 0 relative to first treatment. Results are presented as percentage of baseline, with baseline shown as 100%, fold change from baseline, with baseline shown as 1, or changes in proliferative fraction, indicated as the difference in the %Ki-67$^+$ (Δ%Ki-67$^+$) measured as the designated time points from baseline (0% = no change).

Immunological assays

SIV-specific CD4$^+$ and CD8$^+$ T cell responses were measured in blood and tissues by flow cytometric intracellular cytokine analysis, as previously described (37, 38). Briefly, mixes of sequential (11 amino acid overlapping) 15-mer peptides (AnaSpec) spanning the SIVmac239 Gag, Env, Pol, Nef, Rev, Tat, Vif, Vpr and Vpx proteins were used as antigens in conjunction with anti-CD28 (CD28.2, Purified 500 ng/test: eBioscience, Custom Bulk 7014–0289-M050) and anti-CD49d stimulatory mAb (9F10, Purified 500 ng/test: eBioscience, Custom Bulk 7014–0499-M050). Cells were incubated at 37°C with peptide mixes and antibodies for 1 hour, followed by an additional 8-hour incubation in the presence of Brefeldin A (5 μg ml^{-1}; Sigma-Aldrich). Stimulation in the absence of peptides served as background control. After incubation, stimulated cells were stored at 4°C until staining with combinations of fluorochrome-conjugated mAbs including: anti-CD3 (SP34–2: Pacific Blue; BD Biosciences, Custom Bulk 624034 and PerCP-Cy5.5; BD Biosciences, Custom Bulk 624060), anti-CD4 (L200: FITC; BD Biosciences, Custom Bulk 624044 and AmCyan; BD Biosciences, Custom Bulk 658025), anti-CD8α (SK1: APC-Cy7; eBioscience, Custom Bulk 7047–0087-M002), anti-TNF-α (MAB11: APC; BD Biosciences, Custom Bulk 624076 and FITC; BD Biosciences, Custom Bulk 624046 and PE; BD Biosciences, Custom Bulk 624049), anti-IFN-γ (B27: APC; BD Biosciences, Custom Bulk 624078 and FITC; BD Biosciences, 554700) and anti-CD69 (FN50: PE; eBioscience, Custom Bulk CUST01282 and PE-TexasRed; BD Biosciences, Custom Bulk 624005). Data were collected on an LSR-II flow cytometer (BD Biosciences). Analysis was performed using FlowJo software (Tree Star). In all analyses, gating on the lymphocyte population was followed by the separation of the CD3+ T cell subset and progressive gating on CD4$^+$ and CD8$^+$ T cell subsets. Antigen-responding cells in both CD4$^+$ and CD8$^+$ T cell populations were determined by their intracellular expression of CD69 and either or both of the cytokines IFN-γ and TNF-α. After subtracting background, the raw response frequencies were memory corrected, as previously described (39, 40). Neutralizing Abs against tissue culture-adapted SIVmac251 were measured in luciferase reporter gene assays using TZM-bl cells as previously described (41).

Antibodies

The following antibodies were used in this study: anti-CD3 (SP34–2: Alexa700; BD Biosciences, Custom Bulk 624042 and Pacific Blue; BD Biosciences, Custom Bulk 624034), anti-CD4 (L200: AmCyan; BD Biosciences, Custom Bulk 658025), anti-CD8α (DK25: Pac Blue; DAKO, PB98401–1), anti-CD8α (SK1: PerCP-Cy5.5, AmCyan APC-Cy7; eBioscience, Custom Bulk 7047–0087-M002), anti-CD95 (DX2: PE; Life

Technologies, Custom Bulk CUST00525), anti-CD28 (CD28.2: PE-Texas Red; BD Biosciences, Custom Bulk 624005), anti-CCR5 (3A9: APC; BD Biosciences, Custom Bulk 624046), anti-Ki-67 (B56: FITC; BD Biosciences, Custom Bulk 624046), anti-CD16 (3G8: Pac Blue; BD Biosciences, Custom Bulk 624034), anti-HLA-DR (L243: PE-Texas Red; BD Biosciences, Custom Bulk 624004), anti-CD20 (L27: APC-Cy7; BD Biosciences, Custom Bulk 655118), anti-CD56 PerCP-Cy5.5 (MEM-188 Invitrogen), anti-CD20 APC-Cy7 (L27 BD Biosciences), anti-NKG2A PE (Z199 Beckman Coulter), anti-CD14 FITC (M5E2 BD Biosciences, R&D Systems) and anti-BrdU FITC, APC (B44 BD Biosciences). Anti-CCR7 Biotin (150503) was purchased as purified immunoglobulin from R&D Systems, conjugated to biotin using a Pierce Chemical Co. biotinylation kit, and visualized with anti-streptavidin (Pac Blue; Life Technologies, S11222). Rhesus recombinant anti-IL-15, clone M111 and IgG isotype control mAb were provided through the National Institutes of Health's Nonhuman Primate Reagent Resource Program.

Viral quantification

Plasma SIV RNA was assessed using a real-time RT-PCR assay (threshold sensitivity = 30 SIV gag RNA copies/ml of plasma; interassay Coefficient of Variance ≤ 25%) as previously described (13, 27). RRV DNA was assessed in whole blood essentially as described (42). Specifically, DNA was purified as previously described (43) and approximately 100 ng of purified total DNA was subsequently analyzed by quantitative real-time PCR (qPCR) on an ABI StepOnePlus (Applied Biosystems). DNA primers utilized for the analysis were designed to amplify a segment of RRV ORF3, which encodes the vMIP. The sequence of the TaqMan primers are as follows: vMIP-1, 5-CCTATGGGCTCCATGAGC-3; and vMIP-2, 5-ATCGTCAATCAGGCTGCG-3. The probe sequence is 5-TCATCTGCCGCCACCCGGTTTA-3. RhCMV DNA in BAL was assessed by qPCR amplification of a segment of the RhCMV UL121 gene essentially as previously described (44). Briefly, nucleic acid was purified from samples using a Magnapure Compact instrument (Roche Diagnostics) according to the manufacturer's instructions. Total nucleic acid in the samples was quantified by absorbance at 260 nm using a Nanodrop ND-1000 spectrophotometer. Duplicate 10 μl samples of purified nucleic acid were analyzed using real-time RT-PCR (Primers included forward - GGGCATCCTCAGGATCACAG, reverse - CGACACCAAGAGGGTATGGG and fluorescently labeled probe 6FAM-ACTCCGAAGACCACAAGGACCCACG-TAMRA) and the resulting copies per sample RhCMV UL121 gene were divided by the micrograms of total nucleic acid in the sample. LCV DNA were assessed by real-time RT-PCR. Nucleic acid was purified from whole blood, resuspended in nuclease-free water, and quantified using a Nanodrop ND-1000 spectrophotometer. 100 ng of total DNA were analyzed in duplicate using primers and Taqman probe specific against the LCV IR1 repeat region and Taqman PCR conditions as previously described (45). PCR amplicons encompassing the IR1 region were quantified by spectrophotometry and diluted from 10^6 to 10^1 copies to generate a standard curve for deriving viral copy numbers.

Immunohistochemistry and RNAScope *in situ* hybridization

At euthanasia and concurrent with blood sampling, tissues, including tumor tissues, were harvested and fixed with 4% paraformaldehyde, diluting 32% solution (Electron Microscopy

Sciences) with PBS, overnight at room temperature. The fixative was replaced with 80% ethanol and tissues were paraffin embedded. For immunohistochemistry (IHC), 4μm thick sections were stained. All stained slides were scanned at high magnification (×400) using a whole-slide scanning microscope (Aperio AT2, Leica Biosystems), yielding high-resolution data from the entire tissue section. The scanned slides were analyzed and figures were produced with HALO Image Analysis Software version 2.3 (Indica Labs). For LCV detection in tissues, IHC was performed with the following antibodies: CD20 (clone L26, DAKO, used in 1:400), CD3 (clone SP34–2, BD, 1:400), and Epstein-Barr nuclear antigen 2 (EBNA2) (PE2, Abcam, 1:1600) using the Bond RX platform (Leica Biosystems) according to the manufacturer's protocol. Briefly, tissue sections were baked, deparaffinized, and rehydrated. Epitope retrieval (ER) for CD20 and EBNA2 was performed using Leica ER1 solution (pH 6) while ER for CD3 was performed using Leica ER2 solution (pH 9) heated to 100°C for 20 min. Endogenous peroxidase activity was quenched with hydrogen peroxide prior to addition of primary Ab. The Bond Polymer Red Refine Detection Kit (Leica Biosystems) was used to detect chromogen for EBNA2 whereas ImmPress Excel Amplified HRP Polymer Staining Kit Anti-Mouse IgG (Vector Laboratories) were used for CD3 and CD20. For RRV detection in tissues, RNAscope in situ hybridization was performed using the Bond RX platform (Leica Biosystems) and the RNAscope 2.5L reagent kit (Advanced Cell Diagnostics [ACD]) according to the manufacturer's protocol. Briefly, freshly cut or previously frozen 4 μm thick sections were stained. Following heat-induced epitope retrieval (HIER) (ACD HIER 15 min with ER2 at 88°C) and proteinase digestion (ACD 15 min Protease), the slides were incubated for 2 hours at 40°C with 2.5LS Probe-V-RRV (ACD-ref: 448028) which is targeting R6, PAN, K8, ORF25, ORF73, and ORF74 (46). Amplification steps were performed according to the ACD protocol. The chromogen was detected with the Bond Polymer Red Refine Detection kit (Leica Biosystems).

Statistics

Mixed model, repeated measures analysis of variance (ANOVA), was used for longitudinal outcome measures and to compare the T cell and NK cell dynamics outcome changes between treatment groups (anti-IL-15 Ab (3 times)/anti-IL-15 Ab (8 times)/IgG control Ab) over the time pi. Since in a typical experiment using repeated measures, two measurements taken at adjacent times are more highly correlated than two measurements taken several timepoints apart, optimal covariance structure chosen by Bayesian Information Criteria (BIC) was used to account for within subject correlation. One-way ANOVA was used for the cross-sectional evaluation including T cell and NK cell dynamics in chronic SIV-infected RM prior to IL-15 blockade and at the time of SIV infection. False discovery rate (FDR) correction method for multiple comparison adjustment was applied. Statistical significance was determined at the significant level of 0.05.

RESULTS

Effect of IL-15 inhibition in chronic SIV infection

We have previously established that a 20mg/kg loading dose, followed by biweekly administration of 10mg/kg of rhesusized anti-IL-15 mAb, was sufficient to establish and maintain essentially complete IL-15 signaling inhibition *in vivo* in SIV-uninfected RM (26).

The most dramatic consequence of this inhibition is profound, sustained depletion of NK cells in blood and tissues. In addition, both $CD4^+$ and $CD8^+$ T_{EM} were substantially (~70%) depleted in blood early after the onset of treatment (with little to no depletion of the T_N, T_{CM} or T_{TrM} populations), but whereas essentially complete NK cell depletion was maintained throughout the IL-15 inhibition period, T_{EM} depletion was countered by the onset of massive T_{TrM} and T_{EM} proliferation, which largely restored circulating T_{EM} numbers, even with continued IL-15 inhibition. Tissue T_{EM}, however, remained significantly reduced, and T_{EM} maintained a very high proliferative rate throughout anti–IL-15 treatment, which appeared to be due to development of increased sensitivity of these cells to alternative γ-chain cytokines, particularly IL-7 (26).

In this study, we randomized 18 RM with asymptomatic, chronic-phase SIVmac239 infection (≥196 days after challenge; Supplemental Table 1) to receive either the same anti-IL-15 regimen described above (n=9) or with a matched regimen using an IgG isotype control mAb (n=9), with anti-IL-15 or control IgG treatment administered every two weeks for 10 weeks (Fig. 1A), resulting in at least 12 weeks of potent *in vivo* IL-15 inhibition. Prior to anti-IL-15 or control IgG treatment, both groups of SIV^+ monkeys manifested profound depletion of circulating $CD4^+$ T_M, with sparing of $CD4^+$ T_N and essentially normal numbers of $CD8^+$ T cells and NK cells relative to SIV^- controls (the latter excepting a modest expansion of the $CD16^-CD56^-$ NK cell and the T_{TrM} $CD8^+$ T cell subsets in the SIV^+ RM; Fig. 1B–D). As shown in Fig. 1D, depletion of $CD4^+$ T_M lineage cells was most marked for effector-differentiated T_{TrM} and T_{EM} (which express the CCR5 co-receptor) and all $CD4^+$ T_M subsets manifested elevated frequencies of Ki-67 expression, indicating hyperproliferation and consistent with the quasi-stable high turnover state that characterizes progressive SIV infection (13, 14). $CD8^+$ T_{CM} and T_{TrM} cells were also hyperproliferative in the SIV^+ RM at baseline (Fig. 1C), consistent with persistent generalized immune activation and an ongoing adaptive $CD8^+$ T cell response to SIV infection.

As observed in SIV^- RM (26), the overall NK cell population was profoundly depleted (mean 95% reduction) in the blood of these chronically SIV-infected RM in the first 14 days of anti-IL-15 treatment, with the dominant $CD16^+$ $CD56^-$ “cytotoxic” subset essentially eliminated (98% reduced), and the “minor” $CD16^-$ $CD56^-$ and “regulatory” $CD16^-$ $CD56^+$ subsets reduced by 93% and 82%, respectively (Fig. 2A). The profound depletion of the $CD16^+$ $CD56^-$ NK cells was maintained throughout the treatment period, whereas the level of depletion became more variable for the $CD16^-$ $CD56^-$ and $CD16^-$ $CD56^+$ subsets after day 42. The response of circulating CD8-lineage T cells in SIV^+ RM to anti-IL-15 treatment was also essentially identical to that observed in SIV^- RM (26), with marked initial depletion of the dominant $CD8^+$ T_{EM} subset (75%), the rapid onset of hyperproliferation within both $CD8^+$ T_{TrM} and T_{EM} subsets, and gradual reconstitution of circulating $CD8^+$ T_{EM} to baseline levels while still on continuing anti-IL-15 treatment (Fig. 2B). The effect of anti-IL-15 treatment on the already markedly depleted, circulating $CD4^+$ T_{EM} subset in SIV^+ RM was difficult to resolve as the observed ~73% depletion on day 14 after treatment did not reach statistical significance due to variability in this tiny, residual population (Fig. 2C). However, we did observe significant hyperproliferation of the remaining $CD4^+$ T_{EM} cells (Fig. 2C), suggesting IL-15 blockade had similar effects as observed in SIV^- RM [at the

very least, the induction of the same increased sensitivity of these cells to alternative γ-chain cytokines (26)].

The anti-IL-15-associated proliferative burst of effector-differentiated $CD4^+$ and $CD8^+$ T_M was also observed in BAL (Fig. 2D). Importantly, a total of ~12 weeks of IL-15 inhibition had no effect on the absolute counts in blood of any $CD4^+$ T cell subset or on CD4/CD8 T cell ratios in BAL (Figs. 2B–D), suggesting that IL-15 signaling was not required to maintain $CD4^+$ T cell homeostasis over the 14 weeks of observation. In addition, IL-15 blockade had no effect on plasma viral loads during or immediately following treatment (Fig. 2E), indicating that IL-15 signaling to effector-differentiated $CD8^+$ T cells was dispensable for maintaining the anti-viral effector responses associated with viral load stability (47, 48), and that NK cells have little to no role in determining these viral set points in chronic SIV infection.

Effect of IL-15 inhibition on primary SIV infection

The above described data did not reveal a non-redundant role for IL-15 signaling or NK cells in chronic SIV infection, once viral replication set points and $CD4^+$ T cell homeostasis processes are established. However, it remained possible that IL-15 signaling or NK cells would play an important role in the initial establishment of the plateau-phase quasi-stable steady state. To evaluate this possibility, we sought to determine the impact of IL-15 blockade prior to and during primary SIV infection by implementing a 3-arm study in which two groups of RM received anti-IL-15 at a 20mg/kg initial dose and 10mg/kg at 2-week intervals thereafter, either given only at 6, 4 and 2 weeks prior to infection (**Group A**; short duration treatment group) or from 6 weeks prior to SIV infection to 8 weeks pi (**Group B**; long duration treatment group) (Fig. 3A). A third cohort of RM (**Group C**) was administered an isotype-matched control mAb on the same schedule as the long duration treatment to serve as a control group for both treatment groups. The short duration (treatment-prior-to-infection) arm was designed to assess the effect of pre-establishing the "IL-15 inhibited state" – including NK cell depletion and $CD4^+$ and $CD8^+$ T_{TrM} and T_{EM} hyperproliferation – on viral and lymphocyte dynamics during and after primary infection, while allowing the IL-15 inhibition to wane prior to development of the plateau-phase quasi-steady state at ~day 56 pi (see NK cell and T_{EM} kinetic analysis below). The long duration treatment arm was designed to additionally evaluate the effect of maintaining IL-15 inhibition throughout primary SIV infection – including NK cell depletion, and interference with overall $CD4^+$ and $CD8^+$ T cell homeostasis and with the adaptive T cell response to SIV infection – on SIV viral replication setpoints, $CD4^+$ depletion rates and overall disease progression.

As expected, the 6 weeks of anti-IL-15 treatment of Groups A and B RM prior to SIV challenge resulted in the same changes in NK and T_{EM} dynamics described above (Supplemental Fig. 1), leading to the following differences between the treated (Groups A and B) versus control (Group C) RM at the time of SIV: 1) profound NK cell depletion in blood and tissues, 2) hyperproliferation of $CD4^+$ and $CD8^+$ T_{EM} and $CD4^+$ T_{TrM} in blood, and 3) hyperproliferation of $CD4^+$ T_M in tissues with high representation of T_{EM} and T_{TrM} (lung airspace and bone marrow) (Fig. 3B–E). Of note, $CD4^+$ and $CD8^+$ T_{EM} counts in

blood were not significantly different between treated and control groups (Supplemental Fig. 1), as the 6-week interval between initiation of IL-15 inhibition and challenge was sufficient for the homeostatic regeneration of these populations.

After SIV challenge, cytotoxic ($CD16^+$ $CD56^-$) and minor ($CD16^-$ $CD56^-$) NK cells remained profoundly depleted in blood throughout acute primary infection in both anti-IL-15-treated RM groups. Rebound of these subsets to control group levels occurred between day 56 and 91 pi in Group A RM and between day 112 and 140 pi in Group B RM (Fig. 4A), consistent with full decay of anti-IL-15 activity occurring by 8–10 weeks after the last dose. The small regulatory ($CD16^-$ $CD56^+$) NK cell subset fluctuated after challenge in Group A RM but appeared to largely return to control levels by day 35 pi in this group, whereas in the Group B RM, depletion of this subset was maintained through ~day 56 pi, before slowly reconstituting to control levels by day 130 pi.

$CD8^+$ T_{CM} numbers in blood did not appreciably change in any of the 3 treatment groups after challenge, and all 3 groups showed a similar post-challenge increase in proliferation (Fig. 4B). In the Group C controls, $CD8^+$ T_{EM} counts in blood transiently increased pi (peaking at day 21 pi) associated with a transient burst of proliferation (Fig. 4B). In contrast, $CD8^+$ T_{EM} in Group A and B RM were hyperproliferative prior to SIV infection and this hyperproliferative state did not change pi until waning of the IL-15 blockade (e.g., in concert with NK cell reconstitution), at which time proliferative rates returned to control levels. Group A and B RM did not show any pi increase in $CD8^+$ T_{EM} absolute counts, and indeed, these counts increased with waning of the IL-15 blockade and the associated hyperproliferation. These data indicate that $CD8^+$ T_{EM} response to infection was restricted in the IL-15-deficient environment, perhaps due to a maximally proliferative, high turnover state. $CD8^+$ T_{TrM} manifested an intermediate phenotype between the T_{CM} and T_{EM}, showing statistically significant hyperproliferation, but only a modest restriction in absolute counts that did not achieve statistical significance.

To directly determine the relative rate of turnover of these $CD8^+$ T cell subsets, proliferating cells were BrdU-labeled at day 40–41 pi (BrdU given over 24 hours) and the $\%BrdU^+$ cells in each subset were subsequently followed (with BrdU decay reflecting overall cell turnover including cell death and proliferative dilution). As shown in Fig. 4B, decay of $BrdU^+$ cells among $CD8^+$ T_{CM} was identical in Groups A-C, indicating IL-15 blockade had no effect on the overall turnover of this population. Among $CD8^+$ T_{TrM}, BrdU decay rates appeared slightly faster in the anti-IL-15-treated groups, but this difference did not achieve statistical significance. However, for $CD8^+$ T_{EM}, BrdU decay in the first 2–3 weeks post-labeling was significantly faster in both treated groups relative to controls, confirming rapid turnover of this subset in anti-IL-15-treated RM, and that this high turnover state persists for ~10 weeks after the last anti-IL-15 dose.

We next evaluated whether IL-15 blockade affected adaptive immune responses to SIV infection and the determination of viral load setpoints. As shown in Fig. 5A, the magnitude of the SIV-specific $CD8^+$ T cell response in blood appeared reduced in the anti-IL-15-treated groups but this reduction did not achieve statistical significance. However, the development of SIV-specific $CD8^+$ T cell responses in lung airspace, representing an extra-lymphoid

effector site, was significantly reduced in the anti-IL-15-treated groups during acute primary infection relative to the control group (Fig. 5A). SIV-specific $CD4^+$ T cells were similar in magnitude in blood across Groups A-C, but again, in lung airspace, these responses were reduced in both anti-IL-15-treated groups (Fig. 5B). $CD4^+$ T cell help to B cells did not appear to be affected by anti-IL-15 treatment, as the kinetics and magnitude of the SIVenv-specific antibody response was essentially identical across all the RM groups (Fig. 5C). Taken together, these results suggest that while anti-IL-15 treatment did not block development of SIV-specific $CD8^+$ and $CD4^+$ T cell responses, it did compromise effector cell production and delivery to extra-lymphoid sites, in addition to almost complete ablation of NK cell populations. These effects, however, did not change SIV replication dynamics as there were no significant differences in the timing or magnitude of peak or plateau-phase plasma viral load in Groups A-C (Fig. 5D).

$CD4^+$ T_M depletion is a hallmark of SIV pathogenesis and the onset of overt immunodeficiency in SIV infection is closely linked to homeostatic collapse of $CD4^+$ T_M populations (14). We therefore next asked whether IL-15 blockade affects $CD4^+$ T_M depletion dynamics in Group A-C RM. As expected, $CD4^+$ T_M dynamics in blood post-SIV challenge were dominated by massive depletion and post-depletion hyperproliferation involving all subsets (Fig. 6A). $CD4^+$ T_{CM} numbers were not appreciably different between the 3 treatment groups after challenge and all 3 groups showed a similar post-challenge increase in proliferation. In addition, decay of $BrdU^+$ cells among $CD4^+$ T_{CM} were identical in Groups A-C, confirming that IL-15 blockade has no detectable effect on the turnover of this population, similar to their $CD8^+$ T_{CM} counterparts (Fig. 4A). $CD4^+$ T_{EM} and T_{TrM} were hyperproliferative prior to infection, and this hyperproliferation decayed to control levels by day 14 pi in both subsets, consistent with the massive depletion of $CD4^+$ T cells pi. Following the post-depletion proliferative burst (day 21 pi), proliferation and decay rates of $BrdU^+$ cells among $CD4^+$ T_{TrM} were similar between all 3 treatment groups. In contrast, the $CD4^+$ T_{EM} proliferative burst was delayed in both groups of anti-IL-15-treated RM, before gradually increasing by day 42 pi and remaining elevated for up to 24 weeks. $CD4^+$ T_{EM} BrdU decay rates were also slightly faster in anti-IL-15-treated RM relative to controls, although this difference was only significant at later time points. Despite the hyperproliferation observed among $CCR5^+$ $CD4^+$ T_{TrM} and T_{EM} populations in anti-IL-15-treated RM at time of SIV infection (Supplemental Fig. 1), the rate and extent of CD4 depletion was not appreciably different between the 3 treatment groups (Fig. 6A). Similarly, $CD4^+$ T_M dynamics (depletion, proliferation and turnover) in the extra-lymphoid effector sites of lung airspace and small intestine were not significantly different between the 3 treatment groups (Fig. 6B). Collectively, these results suggest that IL-15 signaling activity does not play a major role in determining $CD4^+$ T_M population stability following primary SIV infection.

IL-15 inhibition accelerates rhesus macaque rhadinovirus virus reactivation from latency

Based on the fact that $CD4^+$ T_M homeostasis was not significantly altered in anti-IL-15-treated RM in comparison to controls, it was unsurprising to observe that IL-15 inhibition during primary SIV infection had no discernable effect on SIV disease progression, as time to end stage disease was not appreciably different between the 3 treatment groups (Fig. 7A).

At necropsy, pathological findings revealed a wide range of lymphoproliferative disorders, including a large fraction of anti-IL-15-treated RM with AIDS-defining B cell lymphomas (Supplemental Table 2), indicating the possible involvement of oncogenic γ-herpesviruses. Indeed, while most captive-bred RM that are not specifically bred and maintained in specific pathogen free colonies are latently infected with γ-herpesviruses such as RRV, incidences of lytic replication and oncogenesis are extremely low, and mainly manifest in the context of immunodeficiency, such as following SIV infection (43). Here we performed a longitudinal assessment of both RRV and LCV DNA in the blood to determine the impact of IL-15 signaling inhibition and the associated loss of NK cells on the control of RRV and LCV replication following primary SIV infection. As shown in Fig. 7B–C, there was a significant decrease in time to RRV reactivation in anti-IL-15-treated RM relative to controls, as measured by the detection of RRV DNA in the blood. RRV DNA levels increased as early as 6 wk pi in group B and ~12 wk pi in group A, in comparison with 24 wk pi in the control group (Fig. 7C). In addition, RRV reactivation was observed in 6 of 8 RM in Group B in comparison to just 3 RM in both Groups A and C. Of note, 3 RM in Group A and 2 RM in Group B with RRV viremia rapidly progressed to AIDS <6 months pi (Fig. 7A). Thus, if RM with rapid disease progression are excluded, then 3 of 4 (75%) RM in Group A and 6 of 6 RM (100%) RM in Group B were shown to have RRV reactivation. In addition, the timing of RRV reactivation was accelerated with anti-IL-15 treatment, as RRV DNA levels in blood reached detectable levels as early as 6 weeks pi in Group B and approximately 12 weeks pi in Group A, in comparison to 24 weeks pi in the control group (Fig. 7C).

In contrast to the dramatic effects of IL-15 inhibition on RRV replication, the impact of anti-IL-15 treatment on LCV replication was negligible. LCV DNA was detectable in the blood prior to SIV infection and while levels increased following primary SIV infection, they were not significantly different between the 3 treatment groups (Fig. 7D). Similarly, anti-IL-15 treatment had minimal effects on rhesus cytomegalovirus (RhCMV), a β-herpesvirus. As shown in Figure 7E, RhCMV DNA in the lung airspace increased transiently in 1 RM in Group A and 3 RM in Group B before returning to baseline levels in most RM by day 154 pi. Collectively, these data suggest that IL-15 signaling activity has differential effects on the immune control of herpesviruses during progressive SIV infection, as a greater proportion of IL-15-inhibited monkeys showed significant increases in RRV but not LCV or RhCMV replication. However, despite the profound effect IL-15 inhibition had on RRV replication, immunohistochemical staining of malignant lymphoma tissues taken at necropsy from RM with confirmed cases of B cell lymphomas revealed high frequencies of EBNA2-positive B cells, indicating predominantly LCV-associated tumorigenesis (Fig. 8A–B and Supplemental Table 3). RRV was not detectable in any of the malignant tissues, despite the fact that 6 of the 9 RM that had diagnosed B cell lymphoma at necropsy had RRV RNA detectable in the spleen (Fig. 8C and Supplemental Table 3).

DISCUSSION

HIV/SIV pathogenesis is driven by viral replication, but the intensity of this replication and its deleterious effects on the host immune system is thought to be determined by dynamic interplay between 1) activation, destruction and homeostasis (or lack thereof) of $CD4^+$ T cells (the major viral target population), 2) inflammation and immune activation, and 3)

immune responses, potentially both innate and adaptive, that counter both HIV/SIV infection and infection with the opportunistic pathogens that ultimately result in AIDS (14, 49, 50). The central role of IL-15 in the development, function and homeostasis of $CD4^+$ and $CD8^+$ memory/effector T cells and NK cells would suggest that this cytokine orchestrates key elements of these outcome-determining processes, and therefore, that its experimental modulation in SIV-infected RM offers an opportunity both to elucidate the relative important of these processes to SIV infection and disease and to determine whether IL-15-targeted therapeutics would be useful in this setting.

Previous work correlating IL-15 expression levels with SIV infection outcome or administering relatively high dose IL-15 or IL-15 super-agonists to SIV-infected monkeys has suggested that IL-15 can, paradoxically, both promote SIV infection and pathogenesis by enhancing viral replication and inflammation and counter SIV infection and pathogenesis by enhancing anti-viral immunity (19, 21, 24, 32). Similarly, in humans, IL-15 has been shown to enhance $CD4^+$ T cell susceptibility to HIV infection and IL-15 levels have been correlated with increasing HIV viremia and inflammation (23, 51), but at the same time, IL-15 has been shown to enhance T/NK cell function (7, 52–54). Correlation analysis and the study of IL-15 biology via pharmacologic IL-15 administration, while informative, do not provide a complete picture of IL-15 biology as the former does not distinguish cause from effect, and the latter is complicated by the use of supraphysiologic doses, which both accentuate responses, and after initial stimulation, engage counterregulatory mechanisms that have the potential to dysregulate subsequent responses (19, 27, 55). To circumvent these limitations, we developed a method for long-term inhibition *in vivo* of IL-15 in RM, using a rhesusized, neutralizing anti-IL-15 mAb, an approach that abrogates function of physiologic IL-15 expression. Using this approach, we previously demonstrated that in SIV-uninfected RM this IL-15 inhibition profoundly and systemically depletes NK cell populations and disrupts $CD4^+$ and $CD8^+$ T_M cell homeostasis by initially (partially) depleting T_{EM} populations, but then eliciting a compensatory homeostatic response (likely mediated by increased sensitivity to other common γ-chain cytokines, in particular IL-7) that stabilized T_{EM} numbers at the cost of sustained T_{TrM} and T_{EM} hyperproliferation (26).

These changes would be expected to substantially, if not completely, abolish any putative viral suppression mediated by NK cells, and possibly, impair viral suppression by $CD8^+$ effector T cells, which would potentially increase viral replication rates. Because proliferating $CD4^+$ T_M cell are both highly infectible and highly virus productive (56), the increased frequency of actively proliferating $CD4^+$ T_M cells induced and maintained by IL-15 inhibition might also amplify viral replication. In addition, since $CD4^+$ T_M cell hyperproliferation is required to maintain normal or reduced $CD4^+$ T_{EM} populations in the absence of SIV infection (26), it is likely that the homeostatic response to SIV-mediated depletion would be less effective in IL-15-inhibited than in control RM, possibly accelerating the homeostatic failure of $CD4^+$ T_{EM} that contributes to the onset of AIDS (14, 49). Strikingly, despite the fact that these changes were documented for at least 14 weeks in chronically SIV-infected RM subjected to IL-15 inhibition, pvl, $CD4^+$ T cell homeostasis in blood and clinical course were not different than in control treated RM, observations strongly suggesting that in the quasi-stable steady state of chronic, asymptomatic SIV

infection, IL-15 signaling is dispensable over a 3-month time frame, and NK cells play a minimal role, if any, in determining plateau-phase viral replication rates.

Immune perturbations during primary SIV infection, prior to establishment of steady-state, tend to have a much bigger impact on SIV pathogenesis than when applied in chronic SIV infection. For example, anti-CD8α mAb-mediated $CD8\alpha^+$ cell depletion (which depletes both $CD8^+$ T cells and NK cells) in primary SIV infection invariably results in sustained excess plasma viremia and rapid disease progression, whereas in chronic SIV infection, similar treatment typically results in only a transient increase in plasma viremia (27, 48, 57). However, when IL-15-inhibited monkeys with the aforementioned characteristic changes of this treatment were infected with SIV, there was again no difference in either peak or plateau-phase plasma viremia or in both blood and tissue $CD4^+$ T_M cell depletion relative to controls, even when IL-15 inhibition was maintained into plateau-phase. Adaptive $CD4^+$ and $CD8^+$ T cell responses to SIV were not significantly impaired in blood of IL-15-inhibited RM, although peak, but not plateau-phase effector frequencies of SIV-specific T cells were significantly, but only partially, reduced in pulmonary airspace, consistent with the described role of IL-15 in promoting memory/effector T cell delivery to extra-lymphoid tissues (17). However, the essentially identical 1.5 log drop in plasma viremia from peak to plateau-phase in both anti-IL-15-treated and control RM groups strongly suggests that anti-viral immunity – to the extent that it is effective in SIV-infected RM – was not impaired with IL-15 inhibition.

This outcome is substantially different from the outcome of nearly universal hyperviremia and rapid progression with $CD8^+$ cell depletion in the same timeframe (27). Both anti-CD8α and anti-IL-15 treatments result in profound NK cell depletion and in $CD4^+$ T_M cell hyperproliferation, but whereas virus-specific $CD8^+$ T cells are only marginally affected by IL-15 inhibition, this population is substantially (if only transiently) depleted by anti-CD8α treatment. These differences imply that $CD8^+$ T cells play the major role in determining acute phase viral dynamics, in particular the drop in post-peak viral loads that protects against rapid progression, with no measurable contribution by either $CD4^+$ T_M cell hyperproliferation or by NK cell-mediated viral suppression. With regard to $CD4^+$ T_M cell hyperproliferation, we have previously demonstrated that $CD4^+$ T_M cell hyperproliferation associated with the anti-CD8α depletion is predominantly IL-15-mediated, and that transient anti-IL-15 treatment can block this hyperproliferation without ameliorating the loss of viral control and accelerated disease progression associated with the anti-CD8α treatment (27).

With regard to NK cell-mediated viral suppression, NK cells have been proposed to contribute to anti-viral effector activity via direct recognition of infected cells by germline-encoded receptors recognizing MHC-related, stress or viral ligands or indirect recognition mediated by anti-viral antibodies binding to the CD16 Fc receptor, resulting in killing of infected cells or viral suppression via elaboration of soluble mediators (58–61). Since many of the NK cell receptor-ligand interactions are highly polymorphic, the best evidence for participation of NK cells in HIV/SIV control is the epidemiologic association of these genetic polymorphisms with viral load set point and/or disease course (29, 62, 63). For example, across multiple HIV^+ cohorts, the combination of the activating killer cell-immunoglobulin (KIR) receptor 3DS1 with HLA *Bw4–80I* correlated with lower HIV

setpoints and improved outcome (63), whereas HLA polymorphisms resulting in higher HLA-E expression (which triggers the inhibitory NKG2A receptor on NK cells) had a deleterious effect on HIV control and disease outcome (29). However, while these correlations are highly significant, the differences in viral loads between groups are quite small, a fraction of a log, far too small to resolve without large population-based cohorts. Thus, if the anti-viral activity of NK cells is limited to these effect sizes, our study would not be powered to resolve these differences. On the other hand, these effects might be the tip of the iceberg, with NK cells playing a broader role in viral control across genetic polymorphisms, perhaps by antibody-dependent cell-mediated cytotoxicity, or perhaps by editing adaptive responses (59, 60). However, our data contradicts this possibility, suggesting that in primary SIV infection of non-vaccinated RM, NK cells have a negligible role in determining viral load dynamics by any mechanism. This result confirms an earlier study which, using CD16 mAb treatment, showed that transient >88% depletion of $CD16^+$ NK cells from blood during primary SIVmac251 infection did not significantly alter pvl dynamics (31). Mathematical modeling of population dynamics following SIV infection also agrees with this conclusion, suggesting that NK cells have little impact on viral load or $CD4^+$ T cell destruction (64).

We have previously proposed that collapse of a quasi-stable homeostasis of $CD4^+$ T_M cell populations, in particular the production and delivery of effector-differentiated $CD4^+$ T_M cells in tissues (T_{EM} and T_{TrM}), precedes and underlies the development of the overt immunodeficiency in SIV-infected monkeys that results in the onset of AIDS (14, 49). Despite the fact that anti-IL-15 treatment partially depletes T_{EM} and induces a hyperproliferative state in the residual T_{EM} and T_{TrM} populations, we saw no significant difference in $CD4^+$ T_M cell depletion dynamics in monkeys with short- or long-term IL-15 inhibition in primary infection vs. controls, nor was there a significant overall difference in time to AIDS between these groups. These data suggest that IL-15 is dispensable for the homeostatic response to $CD4^+$ T cell depletion that stabilizes $CD4^+$ T_M cell numbers above the overt immunodeficiency threshold in the chronic (pre-AIDS) phase of infection, with the caveat that longer treatment intervals and/or larger cohort sizes might have revealed effects that were not discernible in this study.

Herpes family virus reactivation accounts for a significant burden of opportunistic infection in RM AIDS, in particular RhCMV, Rhesus LCV, and RRV (46, 65). Analysis of these viruses in our study RM indicated that LCV replication was similar in IL-15-inhibited vs. control monkeys, and CMV reactivation, though slightly higher in IL-15-inhibited RM (4/15) vs. controls (1/8), was not a dominant infection in either group. However, the onset of RRV reactivation was significantly faster in IL-15-inhibited RM vs. controls, and this reactivation was associated with B cell hyperplasia in treated RM. Interestingly, LCV-associated lymphomas developed in 39% of RM in this study, including 50% of RM given the longer-term anti-IL-15 treatment (vs. 37.5% of control RM). While definitive conclusions cannot be made in this small study, it is tempting to speculate that the loss of IL-15-supported effector populations, in particular NK cells [which are known to be especially important in control of herpesviruses; (66, 67)], combined with $CD4^+$ T_M cell depletion to accelerate the loss of immune control of RRV, possibly also enhancing LCV tumorigenesis by inducing B cell hyperplasia and expanding lytic LCV infection (46, 68).

The possibility that continuation of IL-15 inhibition deeper into chronic phase SIV infection might have further accelerated immunodeficiency will have to be resolved in future studies.

In summary, our results show that inhibition of IL-15-mediated signaling for up to 10 weeks in primary SIV infection and 12 weeks in chronic SIV infection does not materially change viral or $CD4^+$ depletion dynamics in RM. This lack of effect is surprising given the nearly complete NK cell ablation with this treatment, suggesting that NK cells play no role, or at most, a minimal role in SIV control, and that loss of adaptive $CD8^+$ T cell responses almost certainly account for the abrogation of viral control and rapid progression associated with $CD8\alpha^+$ cell depletion in primary infection. Whether this lack of NK cell contribution to SIV control is related to inefficient recognition of SIV-infected cells via the array of germline encoded receptors in RM that govern NK cell triggering or to a mismatch between the location, expansion and migration of NK cells relative to viral infection trajectory (69) remains to be determined, but these results suggest that unless key parameters are different in HIV-infected humans, or that NK cell-targeted vaccines can be developed that dramatically change these parameters, $CD8^+$ T cells remain the most potent cellular immune mechanism for HIV/SIV control. In addition, our data suggest that SIV replication and memory $CD4^+$ T cell depletion dynamics are relatively insensitive to T_M cell hyperproliferation and loss of a single common γ-chain cytokine, respectively.

Supplementary Material

Refer to Web version on PubMed Central for supplementary material.

ACKNOWLEDGMENTS

The authors thank the National Institutes of Health (NIH) Nonhuman Primate Reagent Resource, from whom we obtained the rhesus recombinant anti-IL-15 and rhesus IgG control mAb, the Quantitative Molecular Diagnostics Core of the AIDS and Cancer Virus Program of the Frederick National Laboratory for viral load analyses and D. Montefiori for neutralizing Ab assays. The authors also thank J. Turner, S. Planer, T. Swanson, M. Fischer, and A. Legasse for expert animal husbandry. We also thank J. Estes, D. Siess, M. Reyes, J. Clock, A. Kiddle, N. Hamilton, C. Pexton, C. Xu, W. Brantley, A. Maxwell, M. Lidell, M. Marenco, K. Sheffield, S. Hagen, A. Sylwester, H. Park, B. Varco-Merth, A. Townsend and L. Boshears for technical or administrative assistance.

Grant Support: This work was supported by the NIH, National Institute of Allergy and Infectious Disease (grants R37AI054292 and UM1AI126611–02 [L.J.P.] and P51OD011092 [M. K. A, A.D.L.]) and supported in part with federal funds from the National Cancer Institute (Contract No. HHSN261200800001E [J.D.L.] and R01CA206404 [S.W.]). The content of this publication does not necessarily reflect the views or policies of the Department of Health and Human Services, nor does mention of trade names, commercial products, or organizations imply endorsement by the U.S. Government.

Abbreviations used in this article

RM	rhesus macaque
pi	post-infection
T_N	naïve T cell
T_M	memory T cell
T_{CM}	central memory T cell

T_{TrM}	transitional memory T cell
T_{EM}	effector memory T cell
NHP	nonhuman primate
mAb	monoclonal antibody
RRV	rhesus macaque rhadinovirus
LCV	lymphocryptovirus
RhCMV	rhesus cytomegalovirus

REFERENCES

1. Musso T, Calosso L, Zucca M, Millesimo M, Ravarino D, Giovarelli M, Malavasi F, Ponzi AN, Paus R, and Bulfone-Paus S. 1999 Human monocytes constitutively express membrane-bound, biologically active, and interferon-gamma-upregulated interleukin-15. Blood 93: 3531–3539. [PubMed: 10233906]
2. Neely GG, Robbins SM, Amankwah EK, Epelman S, Wong H, Spurrell JC, Jandu KK, Zhu W, Fogg DK, Brown CB, and Mody CH. 2001 Lipopolysaccharide-stimulated or granulocyte-macrophage colony-stimulating factor-stimulated monocytes rapidly express biologically active IL-15 on their cell surface independent of new protein synthesis. J. Immunol 167: 5011–5017. [PubMed: 11673509]
3. Mattei F, Schiavoni G, Belardelli F, and Tough DF. 2001 IL-15 is expressed by dendritic cells in response to type I IFN, double-stranded RNA, or lipopolysaccharide and promotes dendritic cell activation. J. Immunol 167: 1179–1187. [PubMed: 11466332]
4. Fehniger TA, and Caligiuri MA. 2001 Interleukin 15: biology and relevance to human disease. Blood 97: 14–32. [PubMed: 11133738]
5. Rochman Y, Spolski R, and Leonard WJ. 2009 New insights into the regulation of T cells by gamma(c) family cytokines. Nat. Rev. Immunol 9: 480–490. [PubMed: 19543225]
6. Mueller YM, and Katsikis PD. 2010 IL-15 in HIV infection: pathogenic or therapeutic potential? Eur. Cytokine Netw 21: 219–221. [PubMed: 20719708]
7. Guo Y, Luan L, Patil NK, and Sherwood ER. 2017 Immunobiology of the IL-15/IL-15Ralpha complex as an antitumor and antiviral agent. Cytokine Growth Factor Rev. 38: 10–21. [PubMed: 28888485]
8. Robinson TO, and Schluns KS. 2017 The potential and promise of IL-15 in immuno-oncogenic therapies. Immunol. Lett 190: 159–168. [PubMed: 28823521]
9. Steel JC, Waldmann TA, and Morris JC. 2012 Interleukin-15 biology and its therapeutic implications in cancer. Trends Pharmacol. Sci 33: 35–41. [PubMed: 22032984]
10. Verbist KC, and Klonowski KD. 2012 Functions of IL-15 in anti-viral immunity: multiplicity and variety. Cytokine 59: 467–478. [PubMed: 22704694]
11. Alpdogan O, Eng JM, Muriglan SJ, Willis LM, Hubbard VM, Tjoe KH, Terwey TH, Kochman A, and van den Brink MR. 2005 Interleukin-15 enhances immune reconstitution after allogeneic bone marrow transplantation. Blood 105: 865–873. [PubMed: 15280205]
12. Younes SA, Freeman ML, Mudd JC, Shive CL, Reynaldi A, Panigrahi S, Estes JD, Deleage C, Lucero C, Anderson J, Schacker TW, Davenport MP, McCune JM, Hunt PW, Lee SA, Serrano-Villar S, Debernardo RL, Jacobson JM, Canaday DH, Sekaly RP, Rodriguez B, Sieg SF, and Lederman MM. 2016 IL-15 promotes activation and expansion of CD8+ T cells in HIV-1 infection. J. Clin. Invest 126: 2745–2756. [PubMed: 27322062]
13. Okoye A, Meier-Schellersheim M, Brenchley JM, Hagen SI, Walker JM, Rohankhedkar M, Lum R, Edgar JB, Planer SL, Legasse A, Sylwester AW, Piatak M Jr., Lifson JD, Maino VC, Sodora DL, Douek DC, Axthelm MK, Grossman Z, and Picker LJ. 2007 Progressive CD4+ central

memory T cell decline results in CD4+ effector memory insufficiency and overt disease in chronic SIV infection. J. Exp. Med 204: 2171–2185. [PubMed: 17724130]

14. Okoye AA, and Picker LJ. 2013 CD4(+) T-cell depletion in HIV infection: mechanisms of immunological failure. Immunol. Rev 254: 54–64. [PubMed: 23772614]
15. Lugli E, Goldman CK, Perera LP, Smedley J, Pung R, Yovandich JL, Creekmore SP, Waldmann TA, and Roederer M. 2010 Transient and persistent effects of IL-15 on lymphocyte homeostasis in nonhuman primates. Blood 116: 3238–3248. [PubMed: 20631381]
16. Sneller MC, Kopp WC, Engelke KJ, Yovandich JL, Creekmore SP, Waldmann TA, and Lane HC. 2011 IL-15 administered by continuous infusion to rhesus macaques induces massive expansion of CD8+ T effector memory population in peripheral blood. Blood 118: 6845–6848. [PubMed: 22067383]
17. Picker LJ, Reed-Inderbitzin EF, Hagen SI, Edgar JB, Hansen SG, Legasse A, Planer S, Piatak M Jr., Lifson JD, Maino VC, Axthelm MK, and Villinger F. 2006 IL-15 induces CD4 effector memory T cell production and tissue emigration in nonhuman primates. J. Clin. Invest 116: 1514–1524. [PubMed: 16691294]
18. Conlon KC, Lugli E, Welles HC, Rosenberg SA, Fojo AT, Morris JC, Fleisher TA, Dubois SP, Perera LP, Stewart DM, Goldman CK, Bryant BR, Decker JM, Chen J, Worthy TA, Figg WD Sr., Peer CJ, Sneller MC, Lane HC, Yovandich JL, Creekmore SP, Roederer M, and Waldmann TA. 2015 Redistribution, hyperproliferation, activation of natural killer cells and CD8 T cells, and cytokine production during first-in-human clinical trial of recombinant human interleukin-15 in patients with cancer. J. Clin. Oncol 33: 74–82. [PubMed: 25403209]
19. Ellis-Connell AL, Balgeman AJ, Zarbock KR, Barry G, Weiler A, Egan JO, Jeng EK, Friedrich T, Miller JS, Haase AT, Schacker TW, Wong HC, Rakasz E, and O'Connor SL. 2018 ALT-803 transiently reduces simian immunodeficiency virus replication in the absence of antiretroviral treatment. J. Virol 92 e01748–17. [PubMed: 29118125]
20. Webb GM, Li S, Mwakalundwa G, Folkvord JM, Greene JM, Reed JS, Stanton JJ, Legasse AW, Hobbs T, Martin LD, Park BS, Whitney JB, Jeng EK, Wong HC, Nixon DF, Jones RB, Connick E, Skinner PJ, and Sacha JB. 2018 The human IL-15 superagonist ALT-803 directs SIV-specific CD8(+) T cells into B-cell follicles. Blood Adv. 2: 76–84. [PubMed: 29365313]
21. Watson DC, Moysi E, Valentin A, Bergamaschi C, Devasundaram S, Fortis SP, Bear J, Chertova E, Bess J Jr., Sowder R, Venzon DJ, Deleage C, Estes JD, Lifson JD, Petrovas C, Felber BK, and Pavlakis GN. 2018 Treatment with native heterodimeric IL-15 increases cytotoxic lymphocytes and reduces SHIV RNA in lymph nodes. PLoS Pathog. 14: e1006902. [PubMed: 29474450]
22. Roberts L, Passmore JA, Williamson C, Little F, Bebell LM, Mlisana K, Burgers WA, van Loggerenberg F, Walzl G, Djoba Siawaya JF, Karim QA, and Karim SS. 2010 Plasma cytokine levels during acute HIV-1 infection predict HIV disease progression. AIDS 24: 819–831. [PubMed: 20224308]
23. Swaminathan S, Qiu J, Rupert AW, Hu Z, Higgins J, Dewar RL, Stevens R, Rehm CA, Metcalf JA, Sherman BT, Baseler MW, Lane HC, and Imamichi T. 2016 Interleukin-15 (IL-15) strongly correlates with increasing HIV-1 viremia and markers of inflammation. PLoS One 11: e0167091. [PubMed: 27880829]
24. Mueller YM, Do DH, Altork SR, Artlett CM, Gracely EJ, Katsetos CD, Legido A, Villinger F, Altman JD, Brown CR, Lewis MG, and Katsikis PD. 2008 IL-15 treatment during acute simian immunodeficiency virus (SIV) infection increases viral set point and accelerates disease progression despite the induction of stronger SIV-specific CD8+ T cell responses. J. Immunol 180: 350–360. [PubMed: 18097036]
25. Eberly MD, Kader M, Hassan W, Rogers KA, Zhou J, Mueller YM, Mattapallil MJ, Piatak M Jr., Lifson JD, Katsikis PD, Roederer M, Villinger F, and Mattapallil JJ. 2009 Increased IL-15 production is associated with higher susceptibility of memory CD4 T cells to simian immunodeficiency virus during acute infection. J. Immunol 182: 1439–1448. [PubMed: 19155491]
26. DeGottardi MQ, Okoye AA, Vaidya M, Talla A, Konfe AL, Reyes MD, Clock JA, Duell DM, Legasse AW, Sabnis A, Park BS, Axthelm MK, Estes JD, Reiman KA, Sekaly RP, and Picker LJ. 2016 Effect of Anti-IL-15 Administration on T Cell and NK Cell Homeostasis in Rhesus Macaques. J. Immunol 197: 1183–1198. [PubMed: 27430715]

27. Okoye A, Park H, Rohankhedkar M, Coyne-Johnson L, Lum R, Walker JM, Planer SL, Legasse AW, Sylwester AW, Piatak M Jr., Lifson JD, Sodora DL, Villinger F, Axthelm MK, Schmitz JE, and Picker LJ. 2009 Profound CD4+/CCR5+ T cell expansion is induced by CD8+ lymphocyte depletion but does not account for accelerated SIV pathogenesis. J. Exp. Med 206: 1575–1588. [PubMed: 19546246]

28. Ranson T, Vosshenrich CA, Corcuff E, Richard O, Muller W, and Di Santo JP. 2003 IL-15 is an essential mediator of peripheral NK-cell homeostasis. Blood 101: 4887–4893. [PubMed: 12586624]

29. Ramsuran V, Naranbhai V, Horowitz A, Qi Y, Martin MP, Yuki Y, Gao X, Walker-Sperling V, Del Prete GQ, Schneider DK, Lifson JD, Fellay J, Deeks SG, Martin JN, Goedert JJ, Wolinsky SM, Michael NL, Kirk GD, Buchbinder S, Haas D, Ndung'u T, Goulder P, Parham P, Walker BD, Carlson JM, and Carrington M. 2018 Elevated HLA-A expression impairs HIV control through inhibition of NKG2A-expressing cells. Science 359: 86–90. [PubMed: 29302013]

30. Choi EI, Wang R, Peterson L, Letvin NL, and Reimann KA. 2008 Use of an anti-CD16 antibody for in vivo depletion of natural killer cells in rhesus macaques. Immunology 124: 215–222. [PubMed: 18201184]

31. Choi EI, Reimann KA, and Letvin NL. 2008 In vivo natural killer cell depletion during primary simian immunodeficiency virus infection in rhesus monkeys. J. Virol 82: 6758–6761. [PubMed: 18434394]

32. Huot N, Jacquelin B, Garcia-Tellez T, Rascle P, Ploquin MJ, Madec Y, Reeves RK, Derreudre-Bosquet N, and Muller-Trutwin M. 2017 Natural killer cells migrate into and control simian immunodeficiency virus replication in lymph node follicles in African green monkeys. Nat. Med 23: 1277–1286. [PubMed: 29035370]

33. Orzechowska BU, Powers MF, Sprague J, Li H, Yen B, Searles RP, Axthelm MK, and Wong SW. 2008 Rhesus macaque rhadinovirus-associated non-Hodgkin lymphoma: animal model for KSHV-associated malignancies. Blood 112: 4227–4234. [PubMed: 18757778]

34. Searles RP, Bergquam EP, Axthelm MK, and Wong SW. 1999 Sequence and genomic analysis of a Rhesus macaque rhadinovirus with similarity to Kaposi's sarcoma-associated herpesvirus/human herpesvirus 8. J. Virol 73: 3040–3053. [PubMed: 10074154]

35. Rangan SR, Martin LN, Bozelka BE, Wang N, and Gormus BJ. 1986 Epstein-Barr virus-related herpesvirus from a rhesus monkey (Macaca mulatta) with malignant lymphoma. Int. J. Cancer 38: 425–432. [PubMed: 3017870]

36. Wang F 2001 A new animal model for Epstein-Barr virus pathogenesis. Curr Top Microbiol. Immunol 258: 201–219. [PubMed: 11443863]

37. Hansen SG, Piatak M Jr., Ventura AB, Hughes CM, Gilbride RM, Ford JC, Oswald K, Shoemaker R, Li Y, Lewis MS, Gilliam AN, Xu G, Whizin N, Burwitz BJ, Planer SL, Turner JM, Legasse AW, Axthelm MK, Nelson JA, Fruh K, Sacha JB, Estes JD, Keele BF, Edlefsen PT, Lifson JD, and Picker LJ. 2013 Immune clearance of highly pathogenic SIV infection. Nature 502: 100–104. [PubMed: 24025770]

38. Hansen SG, Piatak M, Ventura AB, Hughes CM, Gilbride RM, Ford JC, Oswald K, Shoemaker R, Li Y, Lewis MS, Gilliam AN, Xu G, Whizin N, Burwitz BJ, Planer SL, Turner JM, Legasse AW, Axthelm MK, Nelson JA, Fruh K, Sacha JB, Estes JD, Keele BF, Edlefsen PT, Lifson JD, and Picker LJ. 2017 Addendum: Immune clearance of highly pathogenic SIV infection. Nature 547: 123–124. [PubMed: 28636599]

39. Hansen SG, Ford JC, Lewis MS, Ventura AB, Hughes CM, Coyne-Johnson L, Whizin N, Oswald K, Shoemaker R, Swanson T, Legasse AW, Chiuchiolo MJ, Parks CL, Axthelm MK, Nelson JA, Jarvis MA, Piatak M Jr., Lifson JD, and Picker LJ. 2011 Profound early control of highly pathogenic SIV by an effector memory T-cell vaccine. Nature 473: 523–527. [PubMed: 21562493]

40. Hansen SG, Vieville C, Whizin N, Coyne-Johnson L, Siess DC, Drummond DD, Legasse AW, Axthelm MK, Oswald K, Trubey CM, Piatak M Jr., Lifson JD, Nelson JA, Jarvis MA, and Picker LJ. 2009 Effector memory T cell responses are associated with protection of rhesus monkeys from mucosal simian immunodeficiency virus challenge. Nat. Med 15: 293–299. [PubMed: 19219024]

41. Todd CA, Greene KM, Yu X, Ozaki DA, Gao H, Huang Y, Wang M, Li G, Brown R, Wood B, D'Souza MP, Gilbert P, Montefiori DC, and Sarzotti-Kelsoe M. 2012 Development and

implementation of an international proficiency testing program for a neutralizing antibody assay for HIV-1 in TZM-bl cells. J. Immunol. Methods 375: 57–67. [PubMed: 21968254]

42. Estep RD, Powers MF, Yen BK, Li H, and Wong SW. 2007 Construction of an infectious rhesus rhadinovirus bacterial artificial chromosome for the analysis of Kaposi's sarcoma-associated herpesvirus-related disease development. J. Virol 81: 2957–2969. [PubMed: 17215283]
43. Wong SW, Bergquam EP, Swanson RM, Lee FW, Shiigi SM, Avery NA, Fanton JW, and Axthelm MK. 1999 Induction of B cell hyperplasia in simian immunodeficiency virus-infected rhesus macaques with the simian homologue of Kaposi's sarcoma-associated herpesvirus. J. Exp. Med 190: 827–840. [PubMed: 10499921]
44. Price DA, Bitmansour AD, Edgar JB, Walker JM, Axthelm MK, Douek DC, and Picker LJ. 2008 Induction and evolution of cytomegalovirus-specific CD4+ T cell clonotypes in rhesus macaques. J. Immunol 180: 269–280. [PubMed: 18097028]
45. Sashihara J, Hoshino Y, Bowman JJ, Krogmann T, Burbelo PD, Coffield VM, Kamrud K, and Cohen JI. 2011 Soluble rhesus lymphocryptovirus gp350 protects against infection and reduces viral loads in animals that become infected with virus after challenge. PLoS Pathog. 7: e1002308. [PubMed: 22028652]
46. Marshall VA, Labo N, Hao XP, Holdridge B, Thompson M, Miley W, Brands C, Coalter V, Kiser R, Anver M, Golubeva Y, Warner A, Jaffe ES, Piatak M Jr., Wong SW, Ohlen C, MacAllister R, Smedley J, Deleage C, Del Prete GQ, Lifson JD, Estes JD, and Whitby D. 2018 Gammaherpesvirus infection and malignant disease in rhesus macaques experimentally infected with SIV or SHIV. PLoS Pathog. 14: e1007130. [PubMed: 30001436]
47. Chowdhury A, Hayes TL, Bosinger SE, Lawson BO, Vanderford T, Schmitz JE, Paiardini M, Betts M, Chahroudi A, Estes JD, and Silvestri G. 2015 Differential impact of in vivo CD8+ T lymphocyte depletion in controller versus progressor simian immunodeficiency virus-infected macaques. J. Virol 89: 8677–8686. [PubMed: 26063417]
48. Schmitz JE, Kuroda MJ, Santra S, Sasseville VG, Simon MA, Lifton MA, Racz P, Tenner-Racz K, Dalesandro M, Scallon BJ, Ghrayeb J, Forman MA, Montefiori DC, Rieber EP, Letvin NL, and Reimann KA. 1999 Control of viremia in simian immunodeficiency virus infection by CD8+ lymphocytes. Science 283: 857–860. [PubMed: 9933172]
49. Grossman Z, Meier-Schellersheim M, Paul WE, and Picker LJ. 2006 Pathogenesis of HIV infection: what the virus spares is as important as what it destroys. Nat. Med 12: 289–295. [PubMed: 16520776]
50. McMichael AJ, Borrow P, Tomaras GD, Goonetilleke N, and Haynes BF. 2010 The immune response during acute HIV-1 infection: clues for vaccine development. Nat Rev. Immunol 10: 11–23. [PubMed: 20010788]
51. Manganaro L, Hong P, Hernandez MM, Argyle D, Mulder LCF, Potla U, Diaz-Griffero F, Lee B, Fernandez-Sesma A, and Simon V. 2018 IL-15 regulates susceptibility of CD4(+) T cells to HIV infection. Proc. Natl. Acad. Sci. USA 115: 9659–9667.
52. Garrido C, Abad-Fernandez M, Tuyishime M, Pollara JJ, Ferrari G, Soriano-Sarabia N, and Margolis DM. 2018 Interleukin-15-stimulated natural killer cells clear HIV-1-infected cells following latency reversal ex vivo. J. Virol 92: e00235–18. [PubMed: 29593039]
53. Younes SA, Talla A, Pereira Ribeiro S, Saidakova EV, Korolevskaya LB, Shmagel KV, Shive CL, Freeman ML, Panigrahi S, Zweig S, Balderas R, Margolis L, Douek DC, Anthony DD, Pandiyan P, Cameron M, Sieg SF, Calabrese LH, Rodriguez B, and Lederman MM. 2018 Cycling CD4+ T cells in HIV-infected immune nonresponders have mitochondrial dysfunction. J. Clin. Invest 128: 5083–5094. [PubMed: 30320604]
54. Shasha D, Karel D, Angiuli O, Greenblatt A, Ghebremichael M, Yu X, Porichis F, and Walker BD. 2016 Elite controller CD8+ T cells exhibit comparable viral inhibition capacity, but better sustained effector properties compared to chronic progressors. J. Leukoc. Biol 100: 1425–1433. [PubMed: 27406996]
55. Frutoso M, Morisseau S, Tamzalit F, Quemener A, Meghnem D, Leray I, Jacques Y, and Mortier E. 2018 Emergence of NK cell hyporesponsiveness after two IL-15 stimulation cycles. J. Immunol 201: 493–506. [PubMed: 29848756]
56. Haase AT 2005 Perils at mucosal front lines for HIV and SIV and their hosts. Nat. Rev. Immunol 5: 783–792. [PubMed: 16200081]

57. Fukazawa Y, Lum R, Okoye AA, Park H, Matsuda K, Bae JY, Hagen SI, Shoemaker R, Deleage C, Lucero C, Morcock D, Swanson T, Legasse AW, Axthelm MK, Hesselgesser J, Geleziunas R, Hirsch VM, Edlefsen PT, Piatak M Jr., Estes JD, Lifson JD, and Picker LJ. 2015 B cell follicle sanctuary permits persistent productive simian immunodeficiency virus infection in elite controllers. Nat. Med 21: 132–139. [PubMed: 25599132]
58. Lanier LL 2008 Evolutionary struggles between NK cells and viruses. Nat. Rev. Immunol 8: 259–268. [PubMed: 18340344]
59. Scully E, and Alter G. 2016 NK Cells in HIV Disease. Curr HIV/AIDS Rep 13: 85–94. [PubMed: 27002078]
60. Florez-Alvarez L, Hernandez JC, and Zapata W. 2018 NK cells in HIV-1 infection: from basic science to vaccine strategies. Front. Immunol 9: 2290. [PubMed: 30386329]
61. Banks ND, Kinsey N, Clements J, and Hildreth JE. 2002 Sustained antibody-dependent cell-mediated cytotoxicity (ADCC) in SIV-infected macaques correlates with delayed progression to AIDS. AIDS Res. Hum. Retroviruses 18: 1197–1205. [PubMed: 12487826]
62. Walter L, and Ansari AA. 2015 MHC and KIR polymorphisms in rhesus macaque SIV infection. Front. Immunol 6: 540. [PubMed: 26557119]
63. Bashirova AA, Thomas R, and Carrington M. 2011 HLA/KIR restraint of HIV: surviving the fittest. Annu. Rev. Immunol 29: 295–317. [PubMed: 21219175]
64. Elemans M, Thiebaut R, Kaur A, and Asquith B. 2011 Quantification of the relative importance of CTL, B cell, NK cell, and target cell limitation in the control of primary SIV-infection. PLoS Comput. Biol 7: e1001103. [PubMed: 21408213]
65. Baskin GB 1987 Disseminated cytomegalovirus infection in immunodeficient rhesus monkeys. Am. J. Pathol 129: 345–352. [PubMed: 2823615]
66. De Pelsmaeker S, Romero N, Vitale M, and Favoreel HW. 2018 Herpesvirus Evasion of Natural Killer Cells. J. Virol 92: e02105–17 [PubMed: 29540598]
67. Chijioke O, Landtwing V, and Munz C. 2016 NK cell influence on the outcome of primary Epstein-Barr virus infection. Front. Immunol 7: 323. [PubMed: 27621731]
68. McHugh D, Caduff N, Barros MHM, Ramer PC, Raykova A, Murer A, Landtwing V, Quast I, Styles CT, Spohn M, Fowotade A, Delecluse HJ, Papoudou-Bai A, Lee YM, Kim JM, Middeldorp J, Schulz TF, Cesarman E, Zbinden A, Capaul R, White RE, Allday MJ, Niedobitek G, Blackbourn DJ, Grundhoff A, and Munz C. 2017 Persistent KSHV Infection Increases EBV-Associated Tumor Formation In Vivo via Enhanced EBV Lytic Gene Expression. Cell Host Microbe 22: 61–73. [PubMed: 28704654]
69. Shang L, Smith AJ, Duan L, Perkey KE, Qu L, Wietgrefe S, Zupancic M, Southern PJ, Masek-Hammerman K, Reeves RK, Johnson RP, and Haase AT. 2014 NK cell responses to simian immunodeficiency virus vaginal exposure in naive and vaccinated rhesus macaques. J. Immunol 193: 277–284. [PubMed: 24899503]

KEY POINTS

- Anti-IL-15 depletes NK cells and disrupts T_{EM} homeostasis in SIV-infected RM
- IL-15 inhibition does not alter SIV replication dynamics or $CD4^+$ T cell depletion
- IL-15 inhibition does accelerate reactivation of an oncogenic γ-herpesvirus

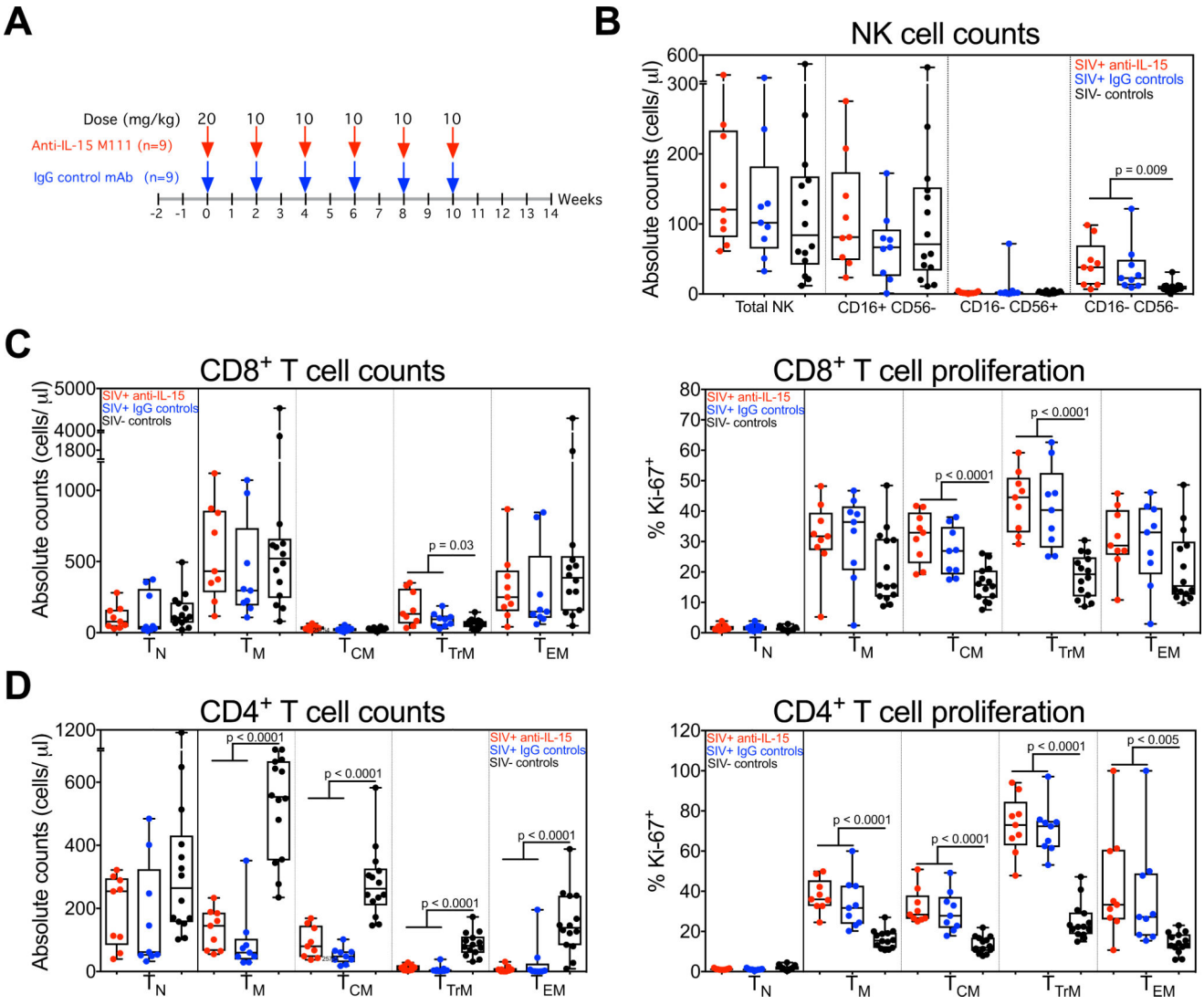

Figure 1. Analysis of T cell and NK cell dynamics in chronic SIV-infected RM prior to IL-15 blockade.

(**A**) A schematic representation of the study protocol showing SIV-infected RM received 20mg/kg of anti-IL-15 or IgG control mAb on day 0 and 10mg/kg on days 14, 28, 42, 56 and 70. (**B**) Comparison of absolute NK cell counts, including $CD16^+$ $CD56^-$, $CD16^-$ $CD56^+$ and $CD16^-$ $CD56^-$ subsets in blood of RM on day 0 of anti-IL-15 mAb treatment (n = 9) or IgG control mAb treatment (n = 9) versus SIV-uninfected control RM (n = 14). (**C**) Comparison of absolute counts and proliferative fraction of $CD8^+$ T cells, including T_N, T_M, T_{CM}, T_{TrM} and T_{EM} subsets in blood of RM on day 0 of anti-IL-15 mAb (n = 9) or IgG control mAb (n = 9) treatment versus SIV-uninfected control RM (n = 14). (**D**) Comparison of absolute counts and proliferative fraction of $CD4^+$ T cells, including T_N, T_M, T_{CM}, T_{TrM} and T_{EM} subsets in blood of RM on day 0 of anti-IL-15 mAb treatment (n = 9) or IgG control mAb treatment (n = 9) versus SIV-uninfected control RM (n = 14). Results are shown as cells/µl of blood for absolute counts or percentage of Ki-67 for proliferation. Each

data point represents a single determination from an individual RM. Significance of difference in all parameters was assessed as described in Materials and Methods.

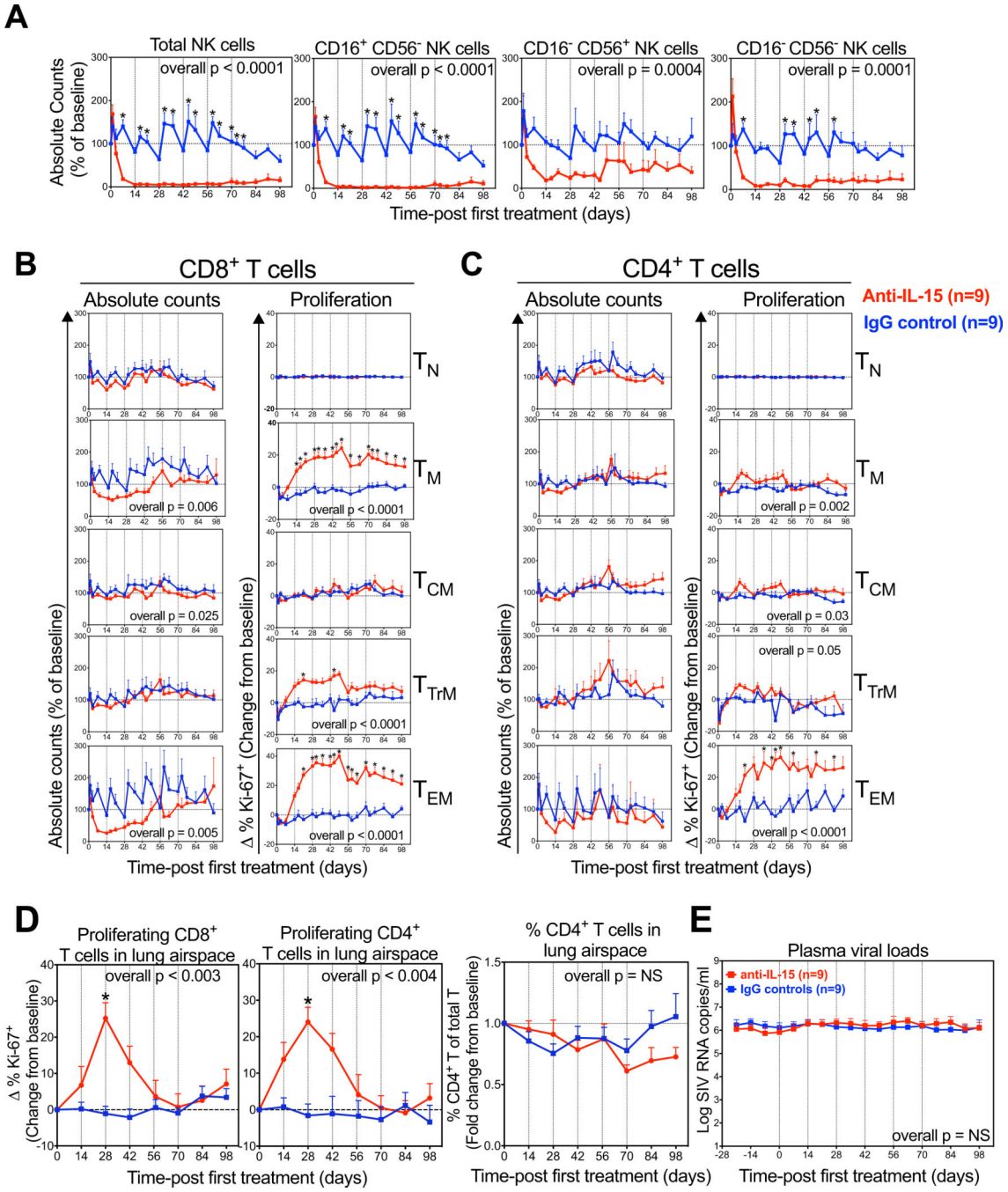

Figure 2. Comparison of NK and T cell dynamics in RM treated with anti-IL-15 during chronic SIV infection.

(**A**) Quantification of absolute NK cell counts, including $CD16^+$ $CD56^-$, $CD16^-$ $CD56^+$ and $CD16^-$ $CD56^-$ subsets in blood after anti-IL-15 mAb (n=9) or IgG control mAb (n=9) treatment. Results (mean + SEM) are shown as percentage of baseline. (**B-C**) Absolute counts and proliferative fraction of $CD8^+$ and $CD4^+$ T cells, including the T_N, T_M, T_{CM}, T_{TrM}, and T_{EM} subsets, in peripheral blood. Results (mean + SEM) are shown as percentage of baseline or for percentage of Ki-67^+, change (Δ) from baseline. (**D**) Proliferative fraction

of $CD8^+$ and $CD4^+$ T cells and percentage of $CD4^+$ T cells of total T cells in lung airspace. Results (mean + SEM) are shown as percentage of $Ki\text{-}67^+$, change (Δ) from baseline or percent $CD4^+$ of baseline. (**E**) Comparison of SIV plasma viral loads after anti-IL-15 mAb (n=9) or IgG control mAb (n=9) treatment. Results (mean + SEM) are shown log SIV RNA copies/ml of plasma. Significance of difference in all parameters was assessed as described in Materials and Methods (*$p < 0.05$).

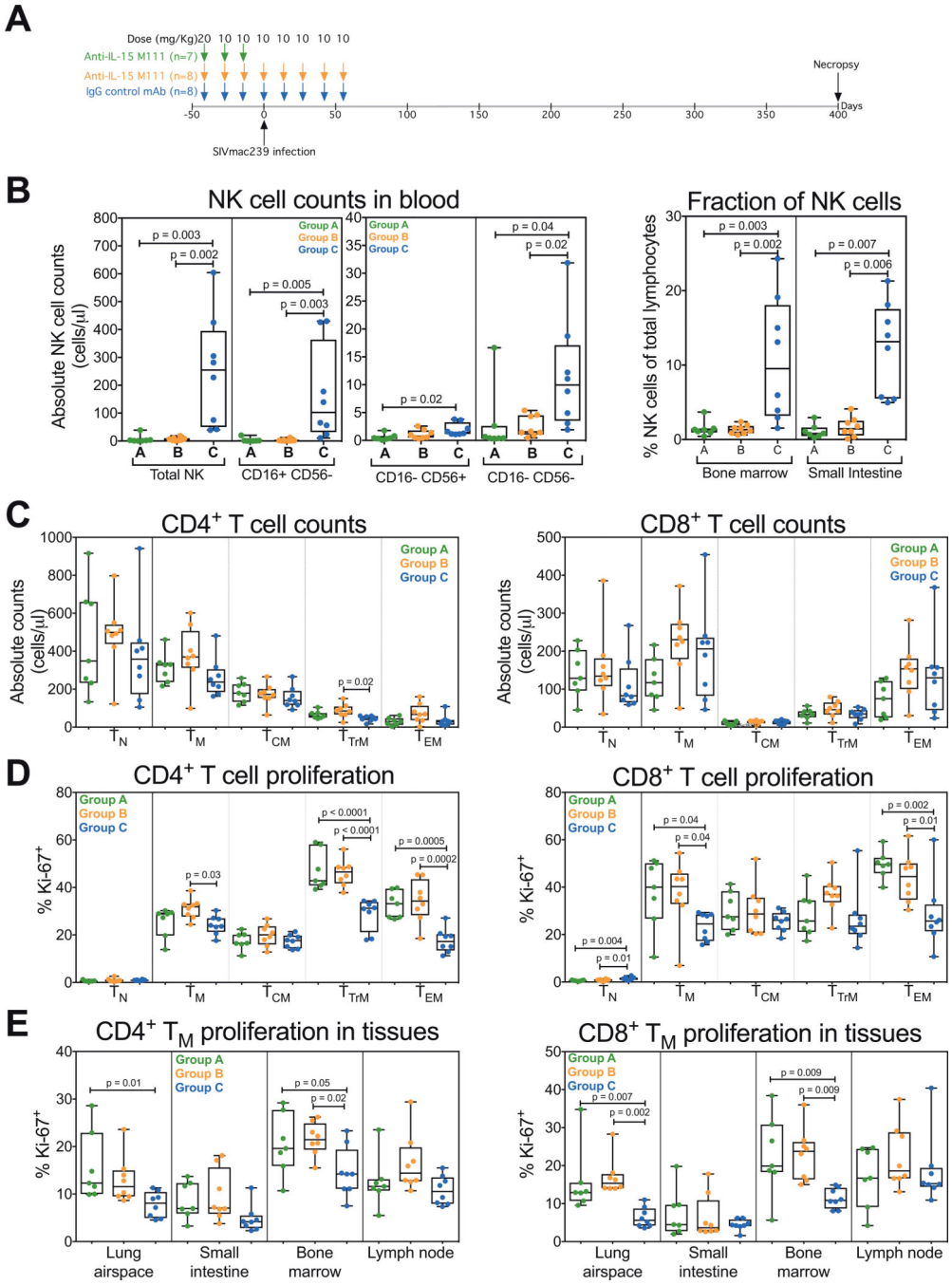

Figure 3. Analysis of NK and T cell dynamics in anti-IL-15-treated RM at time of SIV infection.

(**A**) A schematic representation of the study protocol showing 3 groups of RM received 20mg/kg of anti-IL-15 or IgG control mAb on day −42 and 10mg/kg on days −28 and −14 prior to SIVmac239 infection. Two groups of RM received additional 10mg/kg doses of anti-IL-15 or IgG control mAb on days 0, 14, 28, 42 and 56 post-SIV infection. (**B**) Comparison of absolute NK cell counts, including $CD16^+$ $CD56^-$, $CD16^-$ $CD56^+$ and $CD16^-$ $CD56^-$ subsets in blood and fraction of total NK cells in bone marrow and small intestine on day 0 of SIVmac239 infection in the short duration anti-IL-15 mAb (Group A, n = 7), long

duration anti-IL-15 mAb (Group B, n = 8) or IgG control mAb (Group C, n = 8) treatment groups. (**C-D**) Comparison of absolute and proliferative fraction of $CD4^+$ and $CD8^+$ T cell counts, including T_N, T_M, T_{CM}, T_{TrM} and T_{EM} subsets in blood on day 0 of SIVmac239 infection in each treatment group. (**E**) Comparison of the proliferative fraction of $CD4^+$ and $CD8^+$ T_M in lung airspace, small intestine, bone marrow and lymph node on day 0 of SIVmac239 infection in each treatment group. Results are shown as cells/μl of blood for absolute counts or percentage of Ki-67^+ for proliferation. Each data point represents a single determination from an individual RM. Significance of difference in all parameters was assessed as described in Materials and Methods.

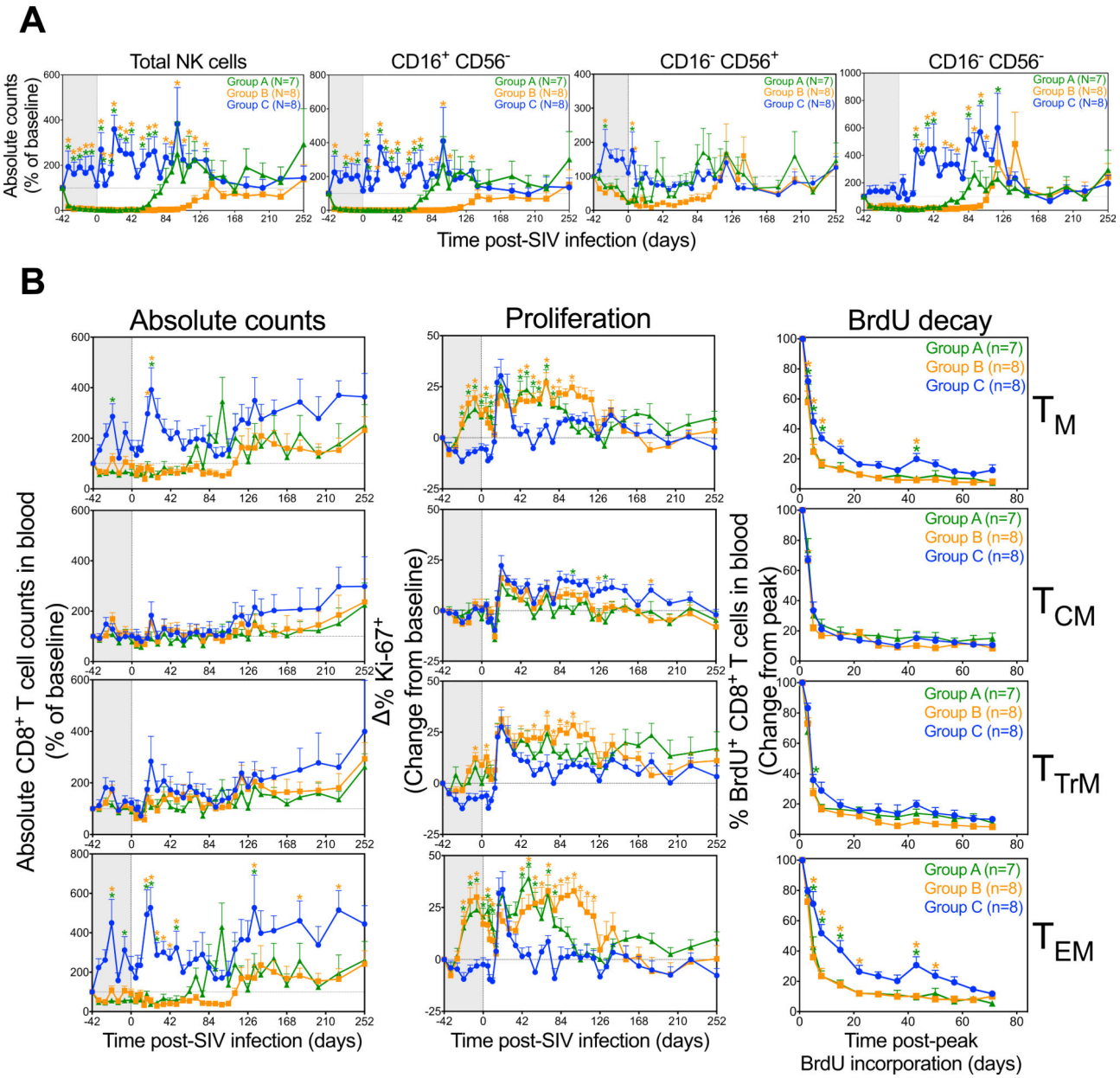

Figure 4. Comparison of NK and CD8$^+$ T cell dynamics in RM treated with anti-IL-15 during primary SIV infection.

(**A**) Absolute NK cell counts, including CD16$^+$ CD56$^-$, CD16$^-$ CD56$^+$ and CD16$^-$ CD56$^-$ subsets in the blood after primary SIVmac239 infection and short duration anti-IL-15 mAb (Group A, n = 7), long duration anti-IL-15 mAb (Group B, n = 8) or IgG control mAb (Group C, n = 8) treatment. Results (mean + SEM) are shown as percentage of baseline. (**B**) RM received three i.v. doses of BrdU at 30 mg/kg over 24 hours between days 40 and 41 pi. Lymphocytes were isolated from the blood or tissues and further analyzed for T cell markers and BrdU positivity. Figure shows comparison of CD8$^+$ T_{CM}, T_{TrM}, T_{EM} and T_N dynamics (absolute counts, proliferative fraction and BrdU decay) in blood after primary SIVmac239 infection and short duration anti-IL-15 mAb (Group A, n = 7), long duration anti-IL-15 mAb

(Group B, n = 8) or IgG control mAb (Group C, n = 8) treatment. Results (mean + SEM) are shown as absolute counts percentage of baseline or percentage of Ki-67^{+}, change (Δ) from baseline or percentage of BrdU^{+}, change from peak. Significance of difference in all parameters was assessed as described in Materials and Methods (*$p < 0.05$).

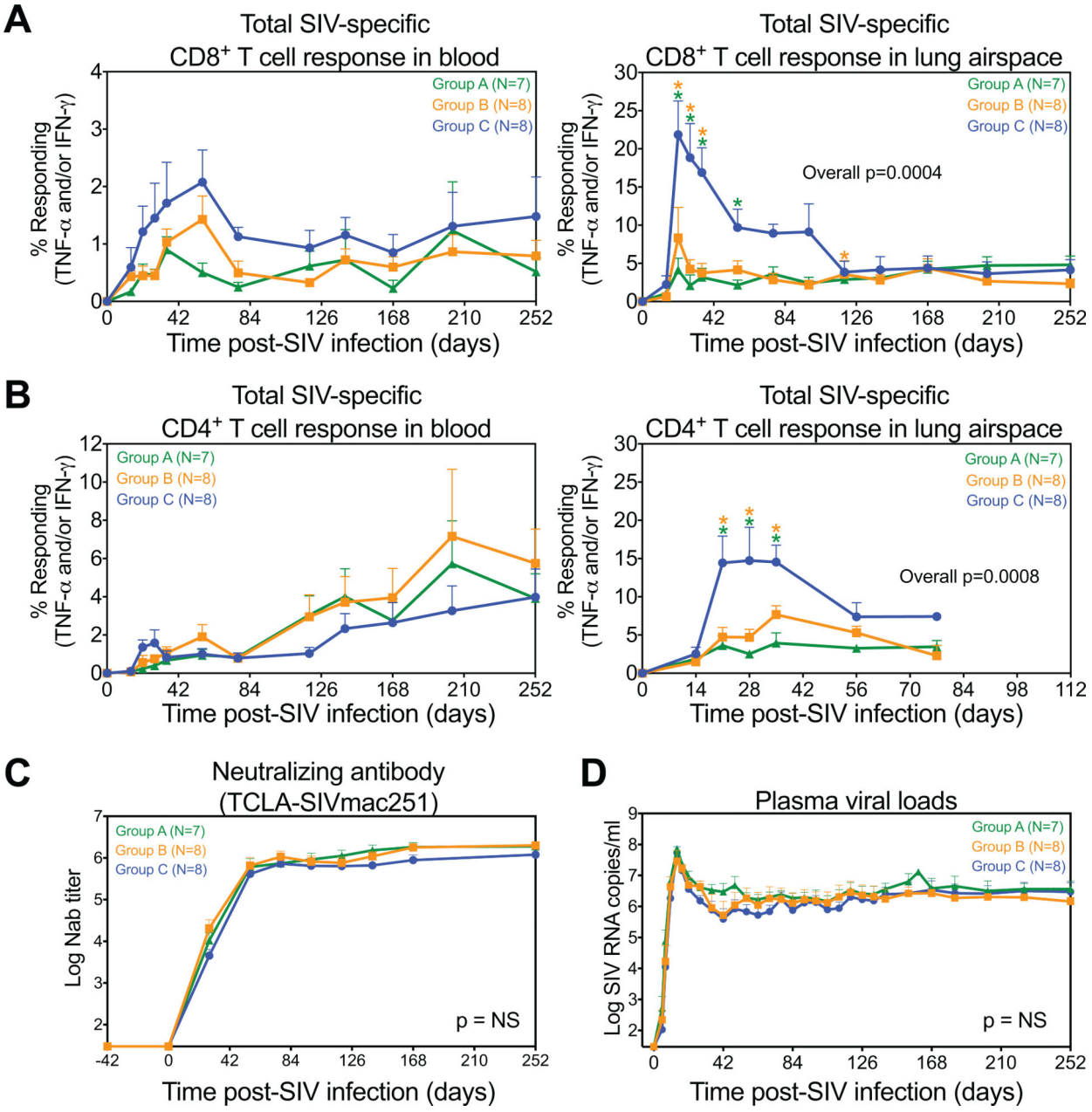

Figure 5. Analysis of SIV-specific immunity in RM treated with anti-IL-15 during primary SIV infection.

(**A-B**) Comparison of $CD8^+$ and $CD4^+$ T cells specific for SIV proteins in blood and lung airspace after primary SIVmac239 infection and short duration anti-IL-15 mAb (Group A, n = 7), long duration anti-IL-15 mAb (Group B, n = 8) or IgG control mAb (Group C, n = 8) treatment. These response frequencies were determined by intracellular expression of TNF-α and/or IFN-γ after stimulation with mixes of consecutive, overlapping SIV 15mer peptides for each SIV protein (Gag, Env, Pol, Nef or protein combinations (Rev/Tat and Vif/Vpr/Vpx), as described in the methods section, with the total response to the SIV proteins expressed by RM reflecting the sum of the Gag, Env, Pol, Nef, Rev/Tat and Vif/Vpr/Vpx responses. Results (mean + SEM) are shown as frequencies of responding

$CD4^+$ or $CD8^+$ T_M. (**C**) Quantification of SIVenv neutralizing antibody responses with results shown as (mean + SEM) log antibody titers in plasma from each treatment group. (**D**) Plasma viral load profiles of RM in each treatment group with results shown as (mean + SEM) log SIV RNA copies/ml of plasma. Significance of difference in all parameters was assessed as described in Materials and Methods (*$p < 0.05$).

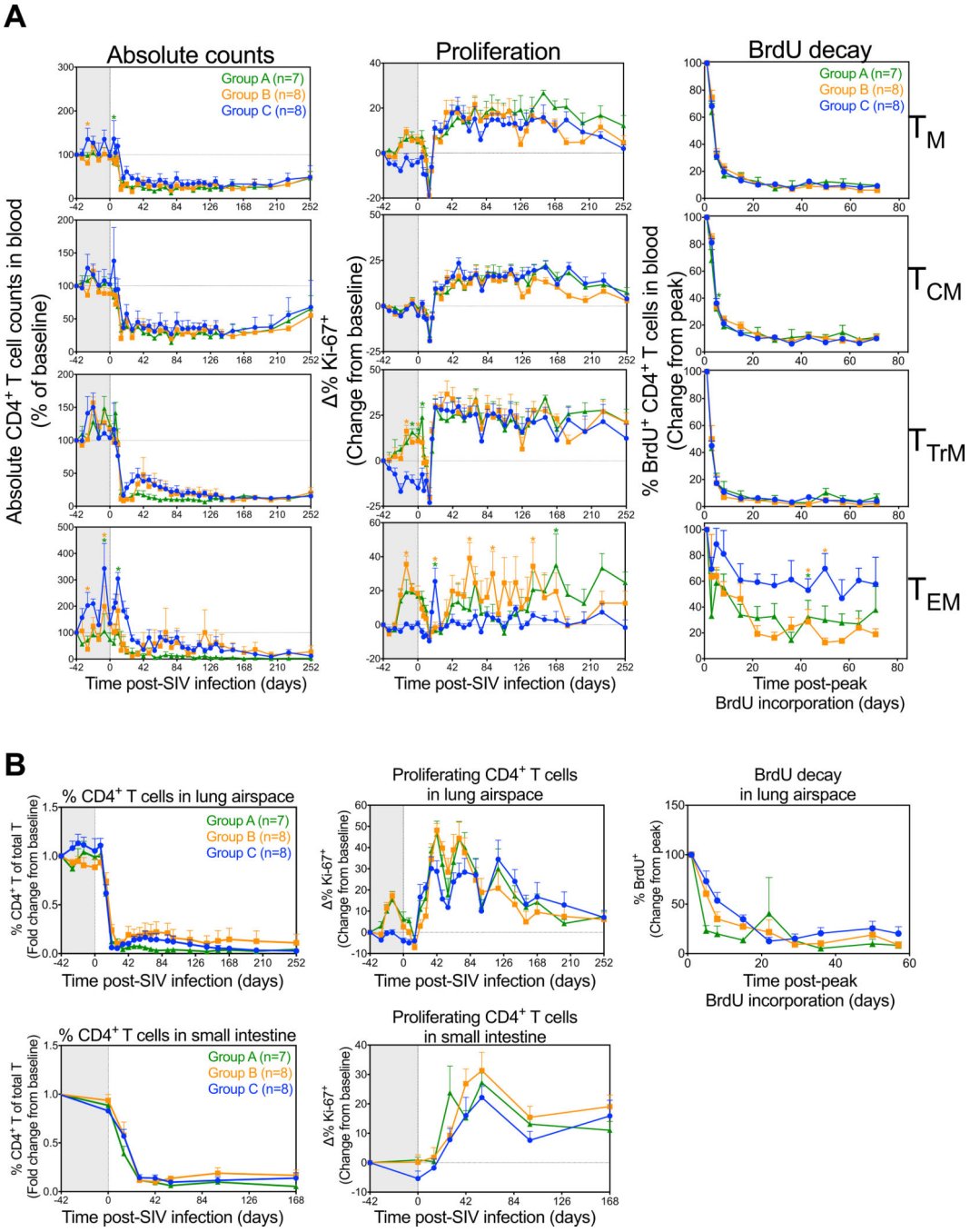

Figure 6. Effects of IL-15 blockade during primary SIV infection on CD4$^+$ T cell dynamics.

(A) Comparison of CD4$^+$ T_{CM}, T_{TrM}, T_{EM} and T_N dynamics (absolute counts, proliferative fraction and BrdU decay curves) in blood after primary SIVmac239 infection and short duration anti-IL-15 mAb (Group A, n = 7), long duration anti-IL-15 mAb (Group B, n = 8) or IgG control mAb (Group C, n = 8) treatment. Results (mean + SEM) are shown as absolute counts percentage of baseline or percentage of Ki-67$^+$, change (Δ) from baseline or percentage of BrdU$^+$ change from peak. (**B**) Comparison of CD4$^+$ T cell dynamics (percentage CD4$^+$ T cells of total T cells, proliferative fraction and BrdU decay curves) in

the lung airspace and small intestine. Results (mean + SEM) are shown as fold change from baseline or percentage of Ki-67$^+$, change (Δ) from baseline or percentage of BrdU$^+$ change from peak. Significance of difference in all parameters was assessed as described in Materials and Methods (*$p < 0.05$).

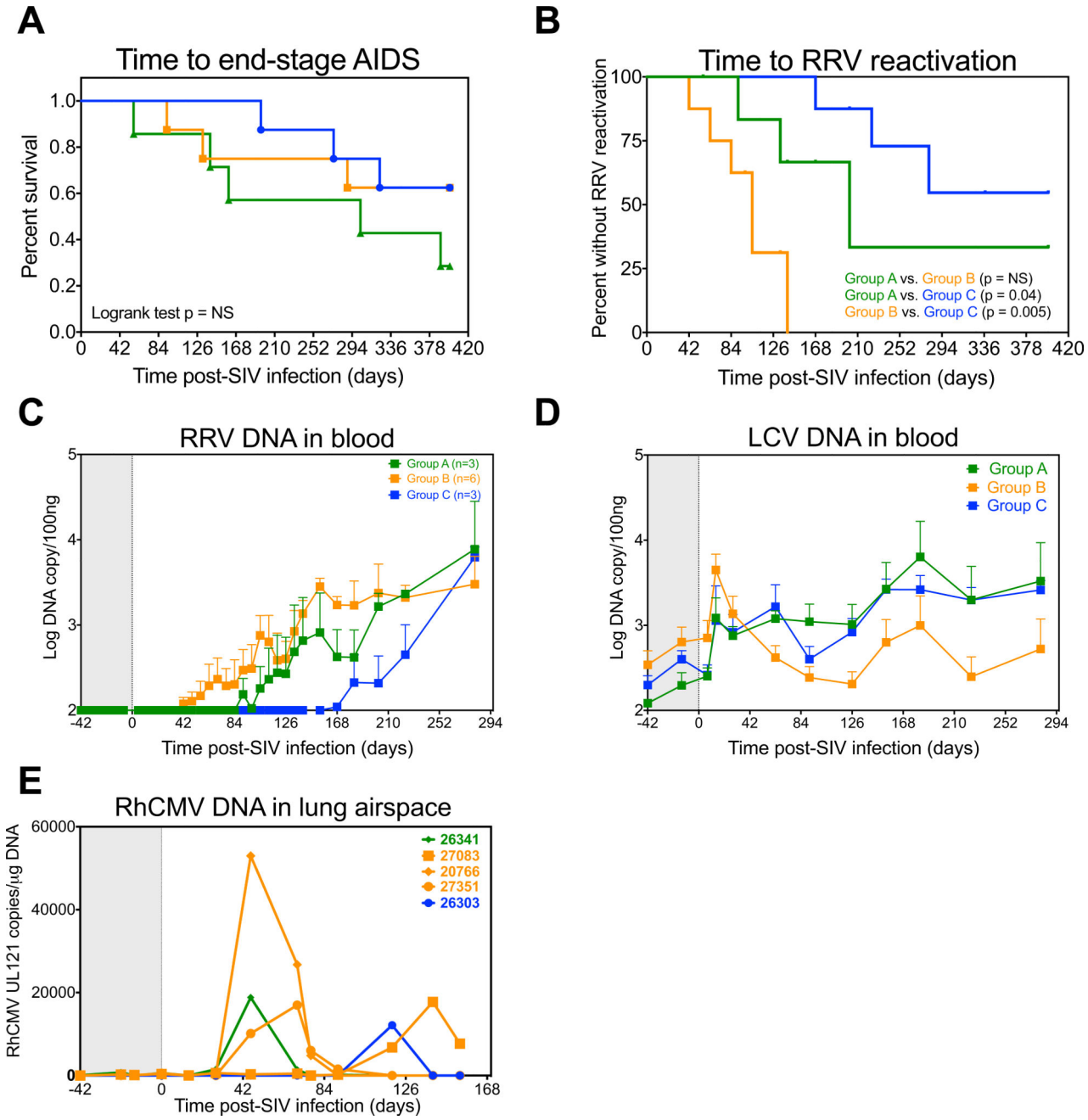

Figure 7. IL-15 blockade during primary infection accelerates RRV reactivation.

(**A**) Kaplan-Meier analysis of time to end-stage disease <400 days post-SIV infection after primary SIVmac239 infection and short duration anti-IL-15 mAb (Group A, n = 7), long duration anti-IL-15 mAb (Group B, n = 8) or IgG control mAb (Group C, n = 8) treatment. (**B**) Kaplan-Meier analysis comparing time to RRV detection in the blood between treatment groups. (**C**) Quantification of RRV DNA in the blood of n = 3 RM in Group A, n = 6 RM in Group B and n = 3 RM in the Group C with RRV reactivation. Results (mean + SEM) are shown as log RRV genome copies/100ng DNA in each RM. (**D**) Quantification of LCV DNA in the blood after primary SIVmac239 infection and short duration anti-IL-15 mAb

(Group A, n = 7), long duration anti-IL-15 mAb (Group B, n = 8) or IgG control mAb (Group C, n = 8) treatment. Results (mean + SEM) are shown as log LCV genome copies/100ng DNA in each RM. (**E**) Quantification of RhCMV loads in lymphocytes isolated from the lung airspace. Results (mean + SEM) are shown as RhCMV UL121 copies/μg of DNA.

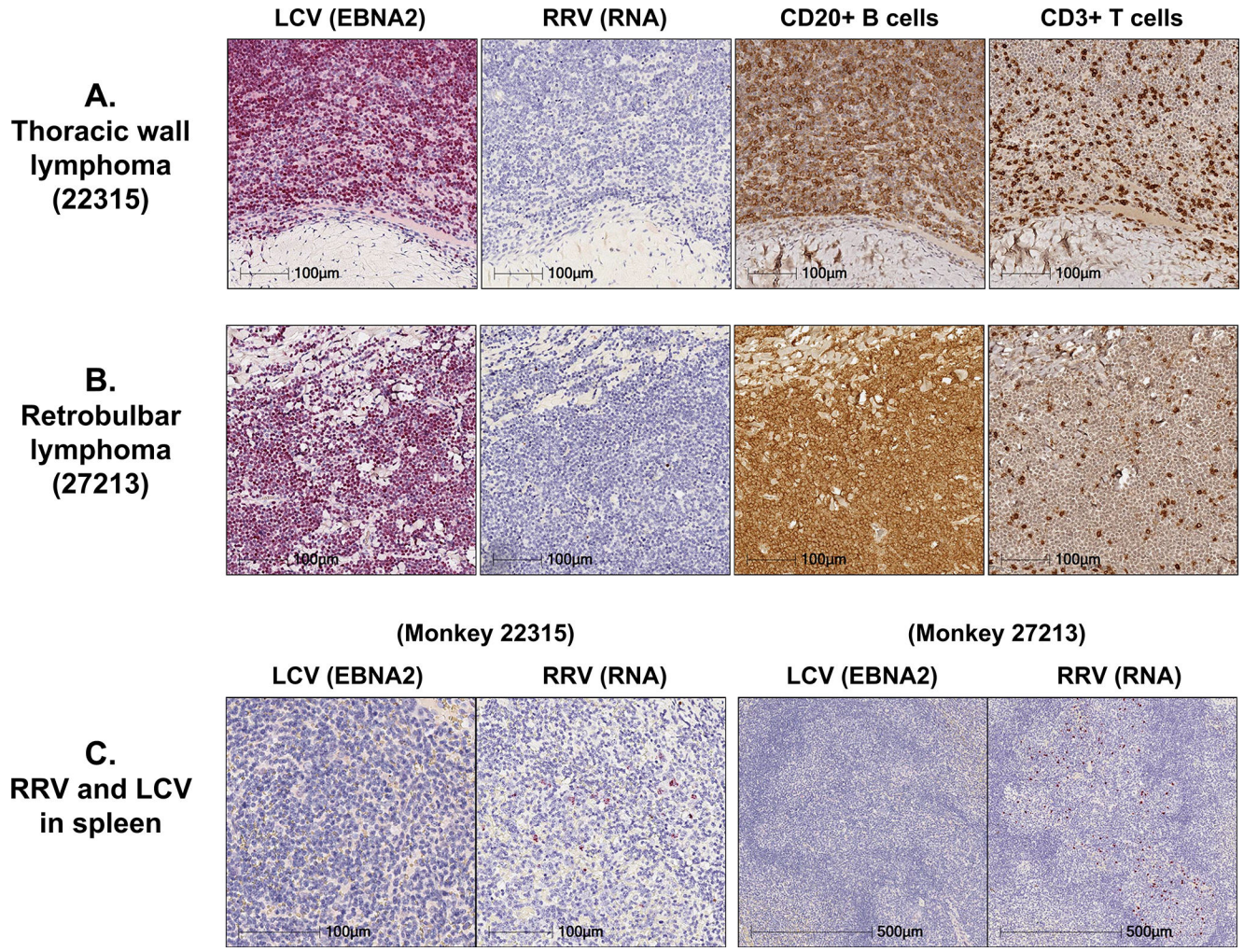

Figure 8. Despite early RRV reactivation, most malignancies were LCV-associated B cell lymphomas.

Representative images of immunohistochemical analysis for EBNA2, CD20, CD3 and RNAscope analysis for RRV RNA performed on (**A**) a thoracic wall lymphoma and (**B**) a retrobulbar lymphoma section obtained from 2 RM that received long duration anti-IL-15 treatment during primary SIV infection and had RRV reactivation in blood. Note high expression of EBNA2 and $CD20^+$ B cells and an almost complete absence of RRV RNA^+ cells in both tissues. (**C**) Representative images showing RRV RNA^+ cells in spleen. RM with RRV reactivation in blood during primary SIV infection also had RRV RNA^+ cells detectable in the spleen, which localized to B cell follicles.